Addis Ababa University
Addis Ababa Institute of Technology
School of Graduate Studies

Development of Rainfall Intensity Duration Frequency Curves for the City of Addis Ababa under the Changing Climate

A thesis submitted and presented to the school of graduate studies of Addis Ababa University in partial fulfillment of the degree of Masters of Science in Civil and Environmental Engineering (Major Water Supply and Environmental Engineering)

BY

LIDEYA ABDISSA

Advisor: Dr. AGIZEW NIGUSSIE

Addis Ababa University
Ethiopia

LIEUABDISSA@GMAIL.COM

October, 2023

Addis Ababa Institute of Technology
School of Graduate Studies

Development of Rainfall Intensity Duration Frequency Curves for the City of Addis Ababa under the Changing Climate

A thesis submitted and presented to the school of graduate studies of Addis Ababa University in partial fulfillment of the degree of Masters of Science in Civil and Environmental Engineering (Major Water Supply and Environmental Engineering)

BY

LIDEYA ABDISSA

Approval by Board of Examiners

Dr. AGIZEW NIGUSSIE	Signature	5/12/2023 Date
Advisor		
DR. MEBRUK MOHAMMED	Signature	5/12/2023 Date
Internal Examiner		
DR. DANEAL F/SILLASIE	Signature	5/12/2023 Date
External Examiner	Abrham Gebre (Dr.) Dean, School of Civil & Environmental Engineering Signature	5/12/2023 Date
DR.ABRHAM GEBRIE		
Chairman (Department of Graduate Committee)	Signature	Date

LIEUABDISSA@GMAIL.COM

DECLARATION AND COPY RIGHT

I, Lideya Abdissa, declare that this is my own original work and all sources of materials used for thesis have been duly acknowledged. This thesis it has not been presented and will not be presented to any other University for similar or any other degree award.

Signature_____

Date_____

Lideya Abdissa

Email Account: - Lieuabdissa@gmail.com

October 2023 Addis Ababa university

ACKNOWELEDGEMENT

First and foremost, I would like to express my sincere gratitude to the Almighty GOD, the most merciful and beneficent, for giving me the gift of life, opportunity to learn and his compassion throughout this study.

I would like to express my deepest and most sincere appreciation to my advisor, Agizew Nigussie (Dr.), for his unwavering guidance, support, and invaluable feedback throughout the research process. His insightful comments and suggestions have been essential in shaping the direction and quality of my work. I am truly blessed to have him as my thesis supervisor and for his friendly and supportive approach.

I would also like to thank to the staff of the National Meteorological Agency (NMA) for providing me with free access to daily rainfall data. I would like to thank Jigjiga University for giving me the opportunity to pursue the MSc studies.

My heartfelt thanks go to my parents, Abdissa Dabale and Buzeyahu Eshatu; My sister Hana Abdissa and my brothers Nati and Eyueal Abdissa for their unwavering love, encouragement, and support as well as for shouldering household responsibility during my coursework and thesis preparation. Their belief in me has been a constant source of strength and motivation.

Finally, I want to thank my husband, Yared Eyob for his unwavering love, encouragement, and support. His patience, understanding, and sacrifice have been instrumental in allowing me to pursue my academic goals. His belief in me has been a source of motivation and inspiration even when I doubted myself. I want to thank him for always being there for me, listening to my thoughts, and helping me see things from a different perspective. I am forever grateful for his presence in my life, and for how he has contributed to my personal and professional growth.

Once again, I want to thank everybody for their direct and indirect contributions to my academic and personal growth.

DEDICATION

This thesis manuscript is dedicated to my family for nursing me with love and affection and for their dedication to support me for the success of my life as well as to my husband **Yared Eyob** and my baby girl (**Zema Yared**) to whom the future Ethiopia belongs.

ABSTRACT

Hydrologic design of water management infrastructures is on the basis of specific design storms derived from historical rainfall events available in the form of intensity-duration-frequency (IDF) curves. However, it is expected that the frequency and magnitude of future extreme rainfalls will change due to the increase in greenhouse gas concentrations in Earth's atmosphere. Developing intensity, duration, and frequency (IDF) of rainfall with the reflection of future climate change is required for designing and managing water infrastructures. Thus, this study presents a rainfall Intensity-Duration-Frequency (IDF) curves for Addis Ababa city under base and climate change scenarios. For this purpose, historical daily rainfall data was collected from Ethiopian National Meteorological Service Agency and bias-corrected CORDEX rainfall data for RCP 8.5 climate scenario was used. Appropriate methods for filling of rainfall data gaps and calculating areal rainfall were employed. Rainfall data tests for independence, stationarity, homogeneity, trend and outliers were also conducted using relevant methods. The data were found to be independent, stationary, homogenous with no trend and outliers. By using EasyFit computer program, the probability distribution that best fits the historical and future rainfall data was selected The Generalized Extreme Value (GEV) distribution was found to be the best fit distribution. Daily historically rainfall and climate scenario data were generated and disaggregated in to hourly basis using the method indicated in ERA Drainage Manual. Expected rainfall quantiles (X_T) for 10min up to 180min durations were computed for return periods of 2, 5, 10, 25, 50, and 100 years using general extreme value (GEV) frequency analysis.

Future Rainfall intensities under climate change scenario RCP8.5 were found to be greater than the historical rainfall intensities by 27%–79% in the period2010-2039; 37%-88% in 2040-2069; and 55%-104% in 2069-2099.; Hence, intense rainfall events are expected in the future and design of stormwater management systems should take this into account.

Keywords: Intensity Duration Frequency Curves, RCP8.5, Climate change, extreme rainfall events, Addis Ababa

Table of Contents

LIST OF TABLES

LIST OF FIGURES

APPENDIX TABLES

APPENDIX FIGURES

LIST OF ABBREVIATIONS AND ACRONYM

AGCMs	Atmospheric General Circulation Models
AOGCM	Atmosphere-Ocean Global Circulation Models
AR4	Fourth Assessment Report
CMIP5	Coupled Model Inter-Comparison Project Phase 5five
CORDEX	Coordinated Regional Climate Downscaling Experiment
CV	Coefficient of Variation
ECDF	Empirical Cumulative Distribution Function
ENMA	Ethiopia National Meteorological Agency
EPCC	Ethiopian Panel on Climate Change
ERA	Ethiopian Road Authority
EV-I	Extreme value Type-I
GCM	General Circulation Model
GEV	Generalized Extreme Value
GHG	Greenhouse Gases
GOF	Goodness of Fit
IDF	Intensity-Duration-Frequency
IDW	Inverse Distance Weighting
IPCC	Intergovernmental Panel on Climate Change
KNN	K-nearest neighbor
MoFED	Ministry of Finance and Economic Development
MoWIE	Ministry of water, irrigation and electricity
NAPA	National Adaptation Program Action in Ethiopia
Net-CDF	Network Common Data Form
OGCMs	Ocean General Circulation Models
RCM	Regional Climate Model
RCP	Representative Concentration Pathways

SRES	Special Report on Emissions Scenarios
SWC	Soil and Water Conservation
TRRL	Transport and Road Research Laboratory
UNFCCC	United Nations Framework Convention on Climate Change
USACE	United States Army Corps of Engineers
USAID	United States Agency International Development
WCRP	World Climate Research Program

1. INTRODUCTION

1.1 Background

Nowadays, environment changes caused by the emanation of ozone-depleting substances have caused an Earth-wide temperature boost and durable changes in all parts of the environmental framework that have a significant effect and can disturb the typical equilibrium of the hydrologic cycle and force a great many effects on the regular and human frameworks on all earthly and marine biological systems of the planet. Assuming the emanation of ozone-harming substances and its related environmental change and fluctuation is gone on in the current style, eventually it will prompt an expanded event of outrageous occasions like weighty downpours, dry spells, and intensity waves. Expectations from environmental models uncovered that the likelihood of concentrated precipitation events will increase from now on.

Increased industrial activity during the last century and a half has increased concentration of carbon dioxide in Earth's atmosphere. This has in turn initiated large scale atmospheric processes resulting in change of global temperature and precipitation (among other variables). Changes in Earth's climate system can disrupt the delicate balance of the hydrologic cycle and can eventually lead to increased occurrence of extreme events (such as floods, droughts, heat waves, summer and ice storms, etc.). For municipalities, changed frequency of extreme events (such as intense rainfall, heavy winds and/or ice storms) are of particular importance as adequate procedures, plans and management strategies must be put in place to deal with them.

Many scientific research conducted on climate change impact including (IPCC) report indicated that there is a change in future meteorological parameters (maximum temperature minimum temperature and precipitation) in different time horizon. One way of reducing vulnerability to adverse impacts of climate change is to anticipate their possible effects, and adapt; the other is to actually reduce the rate of carbon dioxide released into the atmosphere.

According to Ethiopian Panel on Climate Change (EPCC) report, the nation is making remarkable progress in the development of water recourses infrastructure as a means of building sustainable and climate resilient green economy and as a measure of both adaptation to and mitigation of climate change. It is widely recognized that, in the face of climate change, adaptation (i.e.,

adjustment in natural or human systems to moderate harm in response to expected change) is a key mechanism for reducing negative impacts of current and future changes (Kiparsky *et al.*, 2012)

An intensity – duration frequency (IDF) curve is a mathematical function that relates the intensity of an event, such as rainfall, with its duration and frequency of occurrence. in simpler terms, it is a graph that shows how much rain falls in a given amount of time and how often it occurs. The IDF curve is an essential tool for designing and managing water infrastructure such as flood forecasting and urban drainage design.

The IDF curve can take different mathematical expression, either theoretical or empirical fitted to observed event data. For each duration, the empirical cumulative distribution function (ECDF), and a determined frequency or return period is set. Therefore. the empirical IDF curve is given by the union of the points of equal frequency of occurrence and different duration and intensity. The generalized Extreme value (GEV) distribution is often used to fit IDF curves.

Addis Ababa is the biggest city in Ethiopia and home to 25% of the country's metropolitan populace. Populace development filled by provincial movement puts the city poised to double in size in somewhere around 15 years, stressing existing public administrations and usage of rooms. Addis Ababa has an articulated precipitation top during the boreal summer (July to September) and shows the least precipitation during the boreal winter (November to February). The city has a mild environment because of its high elevation in the subtropics. Mean yearly precipitation differs between 730 mm, taking into account authentic information, and 980 mm, taking into account environmental projections. (Giugni M., 2012)

Regarding Addis Ababa, a study was conducted to evaluate the IDF curves for the city under base and climate change scenario. the study employed appropriate methods for filling rainfall data gabs, calculating areal rainfall, and testing rainfall data for independency, stationarity, homogeneity, trend and outliers. the data were found to be independent, stationary, homogeneous with no trend and outliers. The generalized extreme value (GEV) distribution was found to be the best fit distribution by using Easy fit computer program. Daily historical rainfall and climate scenario data were generated and disaggregated into hourly basis using the method indicated in ERA Drainage manual. Expected rainfall quantiles (XT) for 10 min up to 180min durations were computed for return periods.

Climate change can have significance implications for IDF curves. changes in the hydrologic cycle due to increased greenhouse gases causes variation in intensity, duration, and frequency of precipitation events. Quantifying the potential effects of climate change on IDF curves is necessary to reduce urban vulnerability. Reviewing and updating rainfall characteristics such as IDF curve for future climate scenario is necessary.

1.2. Statement of the problem

These days, climate changes brought on by continued greenhouse gas emissions have resulted in global warming and long-lasting changes in all climate system components. These changes can disrupt the hydrologic cycle's normal balance and have a significant impact on both natural and human systems, as well as all terrestrial and marine ecosystems on the planet. Extreme occurrences like torrential rains, droughts, and heat waves will become more frequent if greenhouse gas emissions and the climate change and variability they cause are kept up as they already are. The Intergovernmental Panel on Climate Change (IPCC) findings indicates that developing countries, like Ethiopia, will be more vulnerable to climate change and its ill effects because their economic structure is inflexible and highly dependent on agriculture. Therefore, it is important to understand and predict future changes in temperature and precipitation to effectively manage water resources and their infrastructure.

Flooding due to heavy rainfall is undoubtedly the most disastrous event among the hydro meteorological threats that destroy highways, urban and rural drainage facilities, bridges, hydraulic structures, soil and water conservation (SWC) structures, settlements, and agricultural fields. These days, such events and their consequences are becoming severe in areas like the Addis Ababa city. Therefore, protecting the existing and planning the future urban and rural water management infrastructural components require determination of probable runoff from storms with different magnitude according to the present and projected global and regional climate change and variability.

In water-scarce regions (southern, eastern, and central), increasing evaporation and evapotranspiration, changes in rainfall patterns, and runoff are all projected to increase the frequency of droughts and further diminish availability. The degree of surface water infiltration and groundwater recharge rates are also influenced by variations in rainfall and evaporation, and the nation's reliance on unpredictable rainfall patterns is heightened by inadequate water storage capacity. Changes in rainfall and evaporation translate directly to changes in surface water

infiltration and groundwater re-charge. This has the potential for further decreased reliability of unimproved groundwater sources and surface water sources during droughts or prolonged dry seasons.

Additionally, temperature increases have the potential to result in increased soil moisture deficits even under conditions of increasing rainfall. more intense and frequent storms and flooding may cause storm water flows, which increase the likelihood of water contamination of both surface sources and shallow wells. This is potentially a particularly serious adverse impact as people rely heavily on surface water when wells dry up. Increased temperatures and intense rainfall due to climate change are putting greater pressure on the water and sanitation sector, with potential to further impact development gains.

To have effective and safe water management infrastructures where their design specification relied on rainfall information, providing design standards that consider the impact of changing climate conditions is essential. Hence, in setting every hydrologic design project, determination of the design rainfall that involves an analysis of intensity-duration-frequency (IDF) relationships come first with the consideration of climate change.

Research question

1. Which type of probability distribution best fits the station under consideration in the changing climate?
2. Are IDF curves affected by climate change?
3. What data did you use to develop the IDF curve?
4. What statistical methods did you use to analysis the data and develop the IDF curves?
5. What is the implication of your findings for water resource management and infrastructure planning in Addis Ababa?

1.3. Objectives of the Study

1.3.1. General Objective

The overall objective of this study is to develop rainfall intensity, duration and frequency (IDF) curves that reflect future climate change for designing and managing water infrastructure in Addis Ababa city.

1.3.2. Specific Objectives

Specifically, the study:

- To develop IDF curves for Addis Ababa using historical rainfall data.
- To assess the changes in IDF curves over time
- To project IDF curves for Addis Ababa under RCP 8.5 climate change scenario

1.4. Significance of the Study

Nowadays, human -induced greenhouse gas emissions have brought about a worldwide temperature alteration and dependable changes in all environment framework parts. These progressions can disturb the hydrologic cycle's typical equilibrium and significantly impact ecosystems and human societies, worldwide. Outrageous events like heavy rains, dry seasons, and intensity waves will turn out to be more regular if greenhouse gas emissions continue at their current rate.

The Intergovernmental Board on Environmental Change (IPCC) discoveries show that developing countries, such as Ethiopia, are particularly vulnerable to the impacts of climate change due to their reliance on agricultural and inflexible economies. In this way, understanding and predicting future changes in temperature and precipitation is essential for effective water resource management.

Flooding is the most common and destructive hydro- meteorological hazards, causing damage to infrastructure, settlements, and agricultural land.

In rapidly urbanizing cities like Addis Ababa, flooding is becoming a major concern. The need to protect existing and planned water management infrastructure from flooding is becoming increasingly critical.

1.5. Scope and Limitation of the Study

1.5.1. Scope of the Study

This study is geographically limited to the city of Addis Ababa, Ethiopia. it will focus on the development of the intensity, duration, and frequency of rainfall under climate change using the method recommended by the ERA (2013) drainage design manual. The raw data collected from the Ethiopia national meteorological agency (ENMA) is based on daily base time series.

1.5.2. Limitation of the Study

The study is limited by the lack of available hourly and sub-hourly rainfall records from the Ethiopian Meteorological Agency, which is the main constraint of this research.as a result, it is challenging to disaggregate daily rainfall into sub-hourly amounts necessary for analyzing the IDF

curve. The study is restricted in evaluating other climate variables, such as the mean, maximum, and minimum temperatures of the city.

2. LITERATURE REVIEW

2.1. Climate Change in world

One of the most hotly debated subjects in the most recent climate literature is climate change (literally, if we discuss global warming). The Fourth Assessment Report (AR4) of the Intergovernmental Panel on Climate Change (IPCC), which is the most well-known work on this subject, was released in 2007 (IPCC, 2007a). The IPCC publishes a wide and thorough assessment of climate change every six years.

The variations in rainfall and temperature receive the majority of emphasis in the AR4 and other "climate change" assessments. The IPCC uses the term "climate change" to describe any alteration in the climate over time, whether as a result of cyclical natural phenomena or human activity. Climate change is a term used in the United Nations Framework Convention on Climate Change (UNFCCC) to refer to any change in the climate that is caused by human activity and that modifies the composition of the earth's atmosphere in addition to the natural climatic variability that has been observed over comparable time periods. (IPCC,2014)

According to the IPCC, there is a 95% certainty that human activities are responsible for these rising greenhouse gas concentrations. The main sources of emissions are land use changes, like deforestation to make room for agricultural development to feed a growing population, and emissions from fossil fuels. These greenhouse gases are also absorbed by the oceans, preventing them from remaining in the atmosphere. (IPCC, 2014)

By the middle of the 21st century, the IPCC's Special Report on Managing the Risks of Extreme Events and Disasters to Advance Climate Change Adaptation (IPCC, 2012) predicts that there will almost certainly be more heavy rainfall in eastern Africa and more extremely rainy days. There will also likely be an increase in the frequency of hot days in the future (high confidence), although a decreasing dryness trend over large areas is also projected (medium confidence).

According to the NAPA study, the IPCC's mid-range (A1B) emission scenario predicted that, over Ethiopia, the mean annual temperature will rise by 0.9 to 1.1 °C by 2030, 1.7 to 2.1 °C by 2050, and 2.7 to 3.4 °C by 2080, in comparison to the period from 1961 to 1990. Furthermore, a slight increase in annual precipitation is projected across the country. The principal adverse effects of climate change that the country has already experienced are detailed in the report as a result. Some

of them included food insecurity brought on by droughts and floods; disease outbreaks like malaria, dengue fever, and water-borne illnesses (like cholera and dysentery) brought on by droughts; land degradation as a result of heavy rainfall; and damage to communication, roads, and other infrastructure caused by flooding.

Water resources are just one of the many industries that climate change may have an impact on. Changes in temperature and rainfall patterns, as well as the rising sea level and its effects, are the main contributors. The model simulations predict that rainfall variations will vary across the nation, with some regions receiving more rain and others receiving less. Seasonal patterns and rainfall extremes may also alter Depending on the region, these potential changes have raised worries that, compared to historical experiences, droughts and floods will happen more frequently and/or be more severe under future climate circumstances (IPCC, 2007b).

2.2. Climate model

Climate models simulate the interactions of the atmosphere, oceans, land surface, and ice using quantitative methods. They are employed for a variety of purposes, including researching the dynamics of the weather and climate system and producing future climate projections. The amount of energy entering the earth as short-wave electromagnetic radiation (visible and ultraviolet) and exiting the earth as long-wave electromagnetic radiation (infrared) is balanced or very close to being balanced in all climate models. Any imbalance leads to variations in the planet's average temperature.

Over the past 20 years, significant progress has been made in the creation and application of models, and the available models now provide us with a solid roadmap for the course of future climate change.

One of the best ways to study how climate change affects the environment now is through the use of global circulation models (GCM). These models represent the current state of the art in climate science. To describe how the climate system functions, physics, fluid mechanics, chemistry, and other sciences will be used. Kolbert (2006) asserts that all global circulation models discretize the Earth and its atmosphere into a large number of three-dimensional cells and then apply the relevant equations to those cells.

We can better understand and anticipate the results of greenhouse gas (GHG) emissions by using climate models that relate basic representations of the physical principles governing mass and

energy exchanges in the ocean-atmosphere system. The term "Global Circulation Model" (GCM) is used to describe the mathematical models that are typically used to simulate the current climate and predict future climates with forcing from GHG and aerosols. The most challenging climate models—coupled atmosphere-ocean universal circulation models, or AOGCMs—combine detailed three-dimensional atmospheric general circulation models (AGCMs) with ocean general circulation models (OGCMs), sea-ice models, and models of land-surface processes. For AOGCMs, information about the state of the atmosphere and the ocean closest to, or at, the sea surface is used to compute the interactions of heat, wetness, and energy between the two pieces of equipment (McAvaney *et al.,* 2001).

Most GCMs mimic processes at the continental and global levels and provide a reasonably accurate representation of the average climate. RCMs (Regional Climate Models) dynamically replicate sub-GCM grid-scale climate characteristics using time-varying atmospheric conditions provided by a GCM enclosing a given area. Aerosol dynamics and the carbon cycle might be depicted in the most modern models. The availability of ever-larger and faster computers to run the models coincides with the advancement of these very complex linked models. The largest and most powerful computers on the market are used for climate simulations (Baede et al., 2001). Twenty climate modeling groups from around the world (i.e., the majority of the major organizations conducting climate change research today) met in September 2008 to discuss a new set of coordinated climate model experiments, to be known as phase five of the Coupled Model Inter-comparison Project (CMIP5). Representative Concentration Pathways (RCPs), which are extra emission scenarios, are included in CMIP5 climate models to produce a wide range of outcomes (Moss et al., 2010).

With the publication of the IPCC fifth assessment report (AR5) in September 2013 based on CMIP5 experiment model outputs, it became important to update the prior simulations of expected climate change based on CMIP3 climate models. The CMIP5 typically contains more than 50 advanced climate models (GCMs) from more than 20 modeling centers, in addition to a set of new forcing scenarios known as representative pathways, or RCPs (Taylor et al., 2012).

The latest climate scenarios made accessible to the climate research community are known as Representative Concentration Pathways (RCPs), and they serve as the basis for CMIP5 experiment model simulations. These recently established emission scenarios took into account policies meant to meet a variety of mitigation goals, resulting in different radiative impact by the end of the

twenty-first century. The RCPs are identified based on their potential radiative forcing by the end of the twenty-first century in comparison to the pre-industrial era (1750). The desired radiative forcing values are 2.6, 4.5, 6.0, and 8.5 W/m2, respectively, according to the IPCC (2014). The radiative force estimates provided by each RCP are only indicative of the global radiative forcing by the end of the year 2100.

The RCPs used in AR5 (IPCC Fifth Assessment Report)

The four RCPs that are used in the AR5 (IPCC Fifth Assessment Report) are listed below (Moss R. H *et al.*, 2010).

1. RCP 8.5 – High Emissions

This RCP is consistent with a future with no policy changes to reduce emissions. It was developed by the International Institute for Applied System Analysis in Austria and is characterized by increasing greenhouse gas emissions that lead to high greenhouse gas concentrations over time.

2. RCP 6 – Intermediate Emissions

This RCP was developed by the National Institute for Environmental Studies in Japan. Radiative forcing is stabilized shortly after the year 2100, which is consistent with the application of a range of technologies and strategies for reducing greenhouse gas emissions.

3. RCP 4.5 – Intermediate Emissions

This RCP was developed by the Pacific Northwest National Laboratory in the US. Here, radiative forcing is stabilized shortly after the year 2100, consistent with a future with relatively ambitious emissions reductions.

4. RCP 2.6 – Low Emissions

This RCP was developed by the Netherlands Environmental Assessment Agency. Here, radiative forcing reaches 3.1 W/m2 before returning to 2.6 W/m2 by 2100. In order to reach such forcing levels, ambitious greenhouse gas emissions reductions would be required over time.

2.3. Climate Change in Ethiopia

Ethiopia has the second-highest population on the continent after Nigeria, according to a 2013 list of African countries by population, with 85% of its resident's dependent mostly on agriculture for a living. Due to social, economic, and environmental factors, Ethiopia is particularly vulnerable to the effects of climate change. This nation is more vulnerable to climate change due to a number of variables, including high levels of poverty, rapid population growth, a reliance on rain-fed agriculture, severe environmental degradation, ongoing food insecurity, and recurrent natural drought cycles (NMSA, 2007).

The degree to which Ethiopia is sensitive to the consequences of climate change depends on a number of biophysical and social factors. Ethiopia is known as the "Water Tower of Africa," yet the timely arrival, amount, length, and distribution of rainfall are extremely important to its agricultural sector.

In the report from the Centre for Global Development (CGD, 2011), Ethiopia is ranked eleventh out of 233 countries and other political jurisdictions in terms of their susceptibility to physical climate impacts and ninth in terms of total vulnerability, which considers physical impacts after adjusting for coping capacity.

2.4. impacts of climate change on rainfall in Ethiopia

Ethiopia is referred to as the "water tower" of Northeast Africa and is rich in water resources, with twelve major river basins. However, the nation is unable to take advantage of these plentiful water resources due to its severely inadequate water storage capacity. Abay and Awash River run-off is predicted to decrease by up to one-third due to climate change. The flow into hydropower generating is significantly impacted by a decrease in river runoff. Furthermore, it is anticipated that climate change would cause wetlands to dry up, which may have serious consequences for several bird species' important breeding grounds (World Bank, 2011).

According to NAPA (2011) the water resources sector will be affected by climate change through a decrease in river run-off, a decrease in energy production, as well as increased floods and droughts (the case of Haramaya Lake is notable example).

Water shortages are generally caused by variations in the rainy season, which are a result of climatic variability. As a result, the ecosystem—which provides both rain and water resources— will be impacted. Lack of precipitation would diminish the quantity and quality of a body of water, which would harm aquatic life. For example, a lack of water threatens the fishery, which provides inexpensive protein and causes a food scarcity. Water scarcity will generally cause development projects that depend on water to degrade.

Generally, Ethiopia is vulnerable to the impacts of climate change because of interlinked several factors: poverty, recurrent droughts, high population growth, inequitable land distribution, over exploitation of natural resources, subsistence rain-fed agriculture, etc.

Ethiopia is above all vulnerable to climate change as a consequence of its landscape variability, low income, and bigger dependence on climate susceptible socio-economic sectors such as agriculture, pastoralism and natural resources. Hence, it is very critical to consider the vulnerability

of Ethiopia to climate change impact is a function of several biophysical and socioeconomic factors. (Negussie Ashebir et al. 2015).

2.5.IDF curves under climate change

The Intergovernmental Panel on Climate Change's Fourth Assessment Report (AR4), published in 2007a, makes clearer and more definitive than ever before the existence of climate change. The earth is warming, mostly due to greenhouse gas emissions caused by human activity. The rates of evapotranspiration and rainfall are also varying. One of the main concerns associated with global warming is the influence of hydrological changes (Vo¨ro¨smarty et al. 2000).

Intensity, duration, and frequency of rainfall are predicted to change over time due to climate change. There have never been any alterations to the earth's atmosphere like these. It is clear that the climate system is warming, and many of the changes that have been documented across decades to millennia are unprecedented, according to the Fifth Assessment Report (AR5) of the Intergovernmental Panel on Climate Change. Studies also showed that the projected extreme precipitation, also known as the probable maximum precipitation (PMP), would rise in response to rising temperatures and ensuing increases in atmospheric moisture content. Cities and the infrastructures involved in the management of water resources are greatly impacted by these shifts in extreme climate events, which also have significant ecological, social, and economic effects.

2.6. Rainfall Disaggregation Methods

The majority of climate variables, including rainfall, temperature, wind speed, etc., can be disaggregated. As in previous climate change impact studies, high-resolution rainfall data is necessary for the creation of IDF curves. Rainfall statistics are frequently produced as hourly or lower-resolution statistics. IDF curves, however, are created using sub-hourly, hourly, and daily data. For hydrologic, hydraulic, and all other climate change impact studies, working with the appropriate resolution of climate data is of utmost importance. Due to the constraints of highresolution data measures, it may be difficult to directly obtain high-resolution data for specific regions. The observed data in this study were provided in the daily form, and future data were provided in the daily form. It is difficult to get hourly or sub hourly data from ENMA.

Most meteorological stations do not record rain for shorter periods of time; therefore, GCM outputs are daily. In order to create the 30-min, 1-hour, and other shorter durations needed to generate IDF curves, a practical method of translating 24-hour rainfall depths into rainfall depths of different durations should be implemented.

Disaggregation techniques are widely used, and research documenting disaggregation has been published. There are many models that are utilized, including K-nearest neighbor (KNN) by Prairie et al. (2007), Hyetos by Koutsoyiannis and Onof (2001), and Multivariate Rainfall Disaggregation (MuDRain) by Koutsoyiannis et al. (2003). Some of the methods are detailed in the section below.

Empirical Methods

The Rainfall Ratio Method, developed by the Crothorne, Berkshire-based Transport and Road Research Laboratory (TRRL, 1974) Department of Environment division, can be used to calculate the required amount of rainfall based on a 24-hour rainfall. According to the Ethiopian road authority's 2002 drainage design document, this method was primarily created for use in East African nations while designing roads. The following expression describes the rainfall ratio approach (Fiddes et al., 1974).

$$\frac{Rt}{R24} = \left(\frac{t}{24}\right)\left[\left(\frac{b+24}{b+t}\right)^{n}\right]$$

Where: Rt/R24: Rainfall ratio Rt: Rainfall in a given duration's' (hr) R24: Rainfall in 24 hours, n: constant, b: constant and t: time (hr)

Based on studies of a large number of rainfall gauges in East Africa, the average values of b and n are found to be 0.3 and 0.9, respectively (the range of n is 0.78 to 1.09). The relationship between the daily rainfall amounts and the required short durations is established using regression analysis methods.

K-NN technique

The K-NN technique is a straightforward, non-parametric approach. The method's foundation is resampling from observed data, which highly likely results in the statistical properties of the observed data being preserved in the disaggregated precipitation data (Prodanovic and Simonovic, 2007). Disaggregating precipitation data from a daily scale to hourly and sub-hourly scales in this thesis is a practical strategy due to the ability to preserve the statistical properties of the observed data.

The K-NN technique is a form of nearest neighbor (NN) search, which is also known as closestpoint, similarity, or proximity search. The goal is to identify the most similar or closest

points to the point of interest, where similarity or closeness is measured by Euclidean, Mahalanobis, or other distance metrics (Elshorbagy et al., 2000). The K-NN technique can be defined as follows: If a space S contains a set P of points and a point of interest k is k ∈ S, the K-NN technique finds the closest points (measured by the distance metrics) to k in P (Liu, 2006).

2.7. Frequency Distribution Models

A probability distribution is a function representing the probability of occurrence of a random variable. By fitting a distribution to a set of hydrologic data, a great deal of the probabilistic information in the sample can be compactly summarized in the function and its associated parameters (Chow et al., 1987).

Annual maximum and magnitudes above certain threshold or partial duration series of rainfall data are commonly applied as input for IDF analysis (Ben-Zvi, 2009). Gathering time series records over a range of durations is the first step in the intensity duration frequency analysis. Annual extremes are retrieved from time series data after it has been collected. To estimate rainfall amounts, the annual extreme data is then fitted to a probability distribution. To uniformize the characteristics of rainfall among stations with greatly disparate lengths of record, the probability distribution must fit (Prodanovic and Simonovic, 2007).

There are different distribution functions for IDF analysis: Extreme Value Type I, i.e., Gumbel (EV-I) distribution, generalized extreme value (GEV) distribution, Gamma distribution, Log Pearson III distribution, Lognormal distribution, Exponential distribution [(Koutsoyiannis *et al.*, 1998; Nguyen *et al.*, 2007), recommend Gumbel distribution function and GEV distribution function to be used for IDF analysis. (Prodanovic and Simonovic, 2007) used Gumbel ‘s distribution in constructing IDF curves in two different studies, whereas (Overeem *et al.*, 2008; Hassanzadeh *et al.*, 2014), used the GEV distribution to construct IDF curves due to the superiority of the distribution in describing upper tail behavior.

The goodness of fit (GOF) tests measures the compatibility of a random sample with a theoretical probability distribution function. In other words, these tests show how well the distribution being selected fits to the data. Different GOF criteria ‘s namely; Kolmogorov-Smirnov(K-S), ChiSquared (Shrestha *et al.*, 2017; ERA, 2013), Anderson-Darling(A-D) (ERA, 2013) tests are used for best fitting probability distribution selection. The selection of the best fit method is based on the ranks given by the three criteria (ERA, 2013).

2.7.1. Normal distribution

The normal distribution is a classical mathematical distribution commonly used in the analysis of natural phenomena. The normal distribution has a symmetrical, unbounded, bell-shaped curve with the maximum value at the central point and extending from - ∞ to + ∞. For the normal distribution, the coefficient of skewness is zero. The probability density function (PDF) of this distribution model according to Suresh (2005) is given by:

$$f(x) = S(2\pi)_{0.5} \quad \frac{e^{\frac{(x-x)^{-2}}{2S^2}}}{} \qquad -\propto \leq X \leq \propto \cdots \ldots \ldots \ldots 2.1$$

Note that only two parameters are necessary to describe the normal distribution: the mean value, (x) and the standard deviation, (S). X

The normal distribution has the drawback of being unbounded in the negative direction in contrast to other hydrologic variables, which are finite and can never be less than zero. The normal distribution often has a small number of applications because of this and the fact that many hydrologic variables exhibit a strong skew.

2.7.2. Log-normal distribution

The log-normal distribution has the same characteristics as the normal distribution except that the dependent variable, *X*, is replaced with its logarithm ($Y = log(X)$). The characteristics of the lognormal distribution are that it is bounded on the left by zero and it has a pronounced positive skew. These are both characteristics of many of the frequency distributions that result from an analysis of hydrologic data. The logarithmic transformation of the normal distribution is given as:

$$f(x) = \frac{e^{\frac{(Y-\bar{Y})_2}{2S_Y{}^2}}}{XS_Y(2\pi)_{0.5}} \qquad X > 0 \ldots \ldots \ldots \ldots \ldots \ldots \ldots 2.2$$

Where Y=log(X), Y^- and S_Y are the mean and standard deviation of the sample.

The log-normal distribution has advantage over the normal distribution that it is bounded as x > 0 and the log transformation tends to reduce the positive skewness.

2.7.3. Gumbel extreme value distribution

The most popular probability distribution model for extreme values in hydrologic and meteorological studies, also known as the Gumbel extreme value frequency distribution or the

Gumbel extreme value type I distribution (EVI), has seen the most use for estimating major events in various parts of the world. Studies on rainfall depth, duration, and frequency have made use of this distribution (Garg, 1999).

The Gumbel extreme value type an asymptotic distribution for maximum or minimum events is the limiting mode for the distribution of the maximum or minimum of 'n' independent values from an initial distribution whose right or left tails are unbounded and is an exponential type.

According to Reddi's (2002) theory of maximum events, the probability of the occurrence of an event equal to or larger than a value *Xo* is:

$$P(X \geq X_0) = 1 - e^{-e^{-Y}} \quad \ldots\ldots\ldots\ldots\ldots\ldots\ldots 2.3$$

Where Y=α(X-β) is called the reducer variate. the mean and standard deviation of the variable μ and δ are related to its parameters through the following equations (Reddi. 2002)

$$\alpha = 1.28255/\delta$$
$$\beta = \mu - 0.45005\delta$$

Where α and β are called the parameters of the distribution. the cumulative distribution function is given by

$$F(X) = e^{-e^{-\alpha(x-\beta)}} \qquad -\infty \leq X \leq \infty \ldots\ldots\ldots\ldots\ldots\ldots 2.4$$

$$F(X) = e^{-e^{-Y}} \ldots\ldots\ldots\ldots\ldots\ldots\ldots\ldots\ldots .2.5$$

It may be noted that β is the mode of the distribution point of maximum probability density and 'X' is the variant (historically observed data).

Simplifying and solving equation for Y gives:

$$Y = -\ln\left(ln\left(\frac{1}{F(X)}\right)\right) \ldots\ldots\ldots\ldots\ldots\ldots\ldots\ldots 2.6$$

Substituting of equation yields: - $F(X) = 1 - P \ldots\ldots\ldots\ldots\ldots\ldots\ldots\ldots 2.7$

$$Y = -\ln\left(\ln\left(\frac{1}{1-P}\right)\right) = -\ln\left(\ln\left(\frac{T}{T-1}\right)\right) \ldots\ldots\ldots\ldots\ldots\ldots\ldots 2.8$$

Therefore, for the extreme value distribution, X_T is related to Y_T as follows:

$$Y = \alpha(X - \beta) \rightarrow Y_T = \alpha(X_T - \beta) \ldots\ldots\ldots\ldots\ldots\ldots\ldots .2.9$$

Hence

$$X_T = \beta + \frac{Y_T}{\alpha} \qquad \leftrightarrow X_T = \bar{X} + K_T S_X \ldots\ldots\ldots\ldots\ldots\ldots\ldots\ldots\ldots 2.10$$

2.7.4. Log-Pearson type III distribution

The Gamma distribution has been transformed logarithmically to produce the Log-Pearson type III distribution. A log-Pearson distribution is said to be followed by x if log x follows a Pearson Type III distribution. It has the unique property that the log-Pearson distribution will become the normal distribution when log x is symmetric about its mean. This distribution is widely used in the analysis of rainfall intensities and is the standard distribution for frequency analysis of annual maximum floods. The chi-square test or probability charting can be used to determine whether the distribution fits the data. By Apipattanavis et al. (2005), the probability density function is presented as follows:

$$f(x) = \frac{\lambda\beta(y - \quad)^{\beta-1} e^{-\lambda(y-\varepsilon)}}{x\Gamma(\beta)} \qquad log x \geq \ldots\ldots\ldots\ldots\ldots\ldots\ldots\ldots .11$$

Where $\lambda\ \beta\ and$ are the scale, shape and location parameters of the distribution and y = log x,

$\Gamma(\beta) = (\beta - 1), x = \frac{Sy}{\sqrt{\beta}}$, β $_{(y)} = \left(\frac{2}{\quad}\right)^2_{Cs}$ and $= y - S_y\sqrt{\ }\beta$ assuming the skewness $C_s(y)$ is

positive? the skew coefficient ($C_s(y)$) is determined using the expression:

$$C_s(y) = \frac{n\sum_{i=1}^{n}(y - y)^3}{(n-1)(n-2)(n-3)} \ldots\ldots\ldots\ldots\ldots\ldots\ldots .12$$

Where n is number of observation and the parameters $\lambda\ \beta\ and$ are used to compute the mean μ_y, standard deviation δ_y and coefficient of skew $C_s$of the sample estimates of the population as follows:

$$\mu_y = \quad + \lambda\beta, \qquad \delta_y = \lambda\sqrt{\beta}, \qquad and\ C_s(y) = 2\sqrt{\ }\beta \ldots\ldots\ldots\ldots\ldots\ldots\ldots 13$$

This is referred to as the three-parameter fit. Due to its performance in stochastic hydrology, LogPearson type III distribution has been adopted in a number of countries as a standard distribution for flood frequency analysis.

From the following general equation for any distribution form which the *T*-year event magnitude can be computed: $XT = \mu + K\delta X$

Where *XT is the* event magnitude of the record, μ and δX *are the* mean and standard deviation of the series, and *K* is the frequency factor defined by a specific distribution, is a function of the probability level of *X*.

The log-Pearson type III distribution differs from most of the distributions discussed above in that those three parameters (mean, standard deviation, and coefficient of skew) are necessary to describe the distribution. By judicious selection of these three parameters, it is possible to fit just about any shape of distribution.

2.8. Frequency Analysis Using Frequency Factors

For a given distribution, a relationship can be determined between the frequency factor *(K)* and the return period *(T)*. This relationship can be expressed in mathematical terms or given in a table. The value of *XT* of a hydrologic event may be represented by the mean *(μ)* plus departure of the variate *(Δ XT)* from the mean (Garg, 1999).

$XT = \mu + \Delta XT$

Assuming the departure to be equal to the product of the standard deviation *(δ)* and the frequency factor *KT* (i.e., $\Delta XT = \delta KT$) then, *XT* becomes:

$XT = \mu + KT\,\delta$

The values ΔXT and *KT* are functions of the return period *(T)* and the type of probability distribution to be used in the analysis. If the relationship of the data analysis is in the form of $Y = \log X$, the same style is applied to the statistics for the logarithm of the data using $YT = + KTSY$, and the required value of *XT* is found by taking the antilog of *YT*.

The relationship between the frequency factor *(KT)* and the return period *(T)* is given for different types of distributions as follows (Suresh, 2005):

For normal distribution

$$K_T = \frac{X_T - \mu}{\delta} \quad \ldots\ldots\ldots\ldots\ldots\ldots\ldots 14$$

Where K_T is the same as the standard normal value Z.

For lognormal distribution, the following formula will be used for determining the frequency factor (KT) (U.S. Army Corps of Engineers, 1994; Bhakar *et al.,* 2006):

$$K_T = z = w - \frac{(2.516 + 0.8028w + 0.0103w^2)}{[(1 + 1.4328w + 0.1893w^2 + 0.0013w^3)]} \ldots\ldots\ldots\ldots\ldots\ldots\ldots 15$$

where w is intermediate variable and p is probability of exceedance; w will be calculated using the following formula:

$$w = [\ln (P_{-2})]^{1/2} \qquad (0 < P \leq 0.5) \ldots\ldots\ldots\ldots\ldots\ldots\ldots\ldots 16$$

when p > 0.5, 1- p is substituted for p and the value of z is computed by equation (2.17) is given a negative sign.

For Gumbel Extreme Value Type I distribution, the frequency factor (KT) will be computed by using the following formula (Das, 2004):

$$K_T = \frac{Y_T - \mu_y}{\delta_y} \ldots\ldots\ldots\ldots\ldots\ldots\ldots 17$$

where *YT*, μy, and δy are log transfer of the variable, the mean, and the standard deviation respectively. The value of the reduced variate YT for a given return period T is given as: (Reddi, 2002).

$$Y_T = -\ln [\ln (\frac{T}{T-1})] \ldots\ldots\ldots\ldots\ldots\ldots 18$$

For log-Pearson type III distribution: the frequency factor corresponding to the annual maximum rainfall magnitude as (Suresh, 2005; Adeboye and Alatise, 2007).

$$K_T = z + (z^2 - 1)k + {}^1/_3\,(z^3 - 6z)k^2 - (z^2 - 1)k^3 + zk^4 + {}^1/_3\,k^5 \ldots\ldots\ldots\ldots\ldots 19$$

$$k = \frac{C_s}{6}$$

where KT is frequency factor used for Log Pearson type III distribution, Cs is the coefficient of skewness, and z is standard normal variable or frequency factor (when Cs= 0, then KT = z).

2.9. Intensity – Duration – Frequency Relationships

The determination of the rainfall event or events to be employed is one of the initial steps in many hydrologic design projects, such as urban drainage design. The most popular method is to employ a storm or event that has been designed and has a relationship between the amount of rain, how long it lasts, and how frequently it falls in a certain area, taking into account the facility's location and the return time. The design engineer frequently has readily available for the site standard intensity duration frequency (IDF) curves; therefore, they do not need to carry out this analysis.

The intensity of rainfall decreases with an increase in storm duration. Further, a storm of any given duration will have a greater intensity if the return period is large. In many design problems related to watershed management, such as runoff disposal and erosion control, it is necessary to know the rainfall intensities of different durations and different return periods (Subramanya, 1994).

Through the application of an IDF curve, hydrologists can create hydrologic systems that take the worst-case possibilities for rainfall intensity and duration over a specific period of time into account. Here, it is suggested that heavy rains with high intensity could have disastrous effects. As an illustration, flooding may occur in metropolitan watersheds, resulting in massive volumes of water that the storm water infrastructure is unable to handle. Because of this, proper values for precipitation intensities and frequencies should be taken into account while designing hydrologic systems.

Determining the rainfall event or events to be used is often the initial stage in hydrologic design projects, such as urban drainage planning. The most popular strategy is to use a design storm or event, which involves a relationship between rainfall intensity (or depth), length, and the frequency or return time suitable for the facility and site location. In many circumstances, the hydrologist does not need to undertake this study because the site already has conventional intensity duration frequency (IDF) curves. The IDF is typically displayed as a graph, with each curve representing a design return period and duration and intensity plotted on the horizontal and vertical axes, respectively (Chow, 1988).

Graphs representing the amount of water that falls over a specific region in a given amount of time are frequently provided as curves. When a specific storm is described as a 2-hour, 100-year storm,

it signifies that the storm will endure for two hours (length) and that its frequency in that area will only be equaled or exceeded once every hundred years. It is easy to calculate the amount of rainfall (intensity) for a given location during that time period after you have an understanding of the relevance of each curve.

2.10. Related studies on IDF CURVE in Ethiopia

In the past, different researchers have done analyses on rainfall intensity, duration, and frequency under climate change for different parts of the country. Some of these research works include: IDF under climate change relationships which have been developed for Omo-Gibe basin (Wozader Wolde, 2018), central highland of Ethiopia (Chemeda, 2014), on the upper Blue Nile River basin (Nigatu Merra, 2011). All This study will try to show the impacts of climate change and indicate how procedures and methods should be applied to cope with the problem.

The analysis of the Omo-Gibe basin IDF curve under a changing climate The Omo-Gibe-Giben had received a mean annual rainfall amount between 1046.1 and 1891.2 mm per year for the last decades. Generally, in the three scenarios (RCP 2.6, RCP 4.5, and RCP 8.5), relatively less mean annual rainfall is expected over the Omo-Gibe basin when compared with the baseline period (Wozader W, 2018).

The analysis of the central highlands of Ethiopia uses climate change under the A2a and B2a scenarios. The impacts of climate change were observed by increasing the magnitude of rainfall intensity for a range of durations and return periods. Both SERS emission scenarios (A2a and B2a) indicate that the rainfall magnitude will likely increase in the future, which indicates that climate change is real.

3. MATERIALS AND METHODS

3.1. Description of the Study Area

Addis Ababa is found between $8^0$50' N to $9^0$50' N and $38^0$38 E to $38^0$54' E. It is the capital and the largest city of Ethiopia, with a total projected population of 3.44 million people in 2017. The city is overlooked by Mount Yarer to the east, which is approximately the same height as Mount Entoto, and Mount Wochecha to the west, which is approximately 3361 m above sea level.

Addis Ababa has a pronounced rainfall peak during the boreal summer (July to September) and exhibits a rainfall minimum during the boreal winter (November to February). The city has a temperate climate due to its high-altitude location in the subtropics.

The administration of the city is divided into 11 sub-cities. Addis Ababa is home to 25% of the urban population in Ethiopia and is one of the fastest-growing cities in Africa. It is the growth engine for Ethiopia and a major pillar in the country's vision to become a middle-income, carbonneutral, and resilient economy by 2025. The city alone currently contributes approximately 50% to the national gross domestic product, highlighting its strategic role within the overall economic development of the country (World Bank,2015).

The city is located in the central highlands of Ethiopia, covering an area of about 527 km2 with an average elevation of 2600 m above mean sea level (asl). The altitude range extends from the highest peak at Mount Entoto, which is 3041 m high, to 2051 m above mean sea level at the lower part of the Akaki plain. The average maximum temperature for Addis Ababa over the last 60 years was 22.90 °C, and the average minimum temperature was 10.20 °minimum and maximum temperatures show increasing trends from 1951 to 2002 of 0.4 °C per decade and 0.2 °C per decade, respectively; however, there was no major shift in annual and seasonal rainfall during the period 1898–2002 (Conway,2004). The average annual rainfall in Addis Ababa is 1184 mm. The wet season is from June to mid-September. The urban area is endowed with three major rivers: Kebena, Little Akaki, and Big Akaki, as well as numerous small streams. The population density varies between sub-cities. The highest density is in Addis Ketema sub-city (37,215 people per square kilometer). The lowest density is in Akaki Kality sub-city (1832 p/sk.km). All the sub-cities in downtown have a high population density compared to sub-cities found in peripheral areas. A fast rate of urban

expansion is occurring, and built-up areas are rapidly increasing in Addis Ababa (Woldegerima,2016).

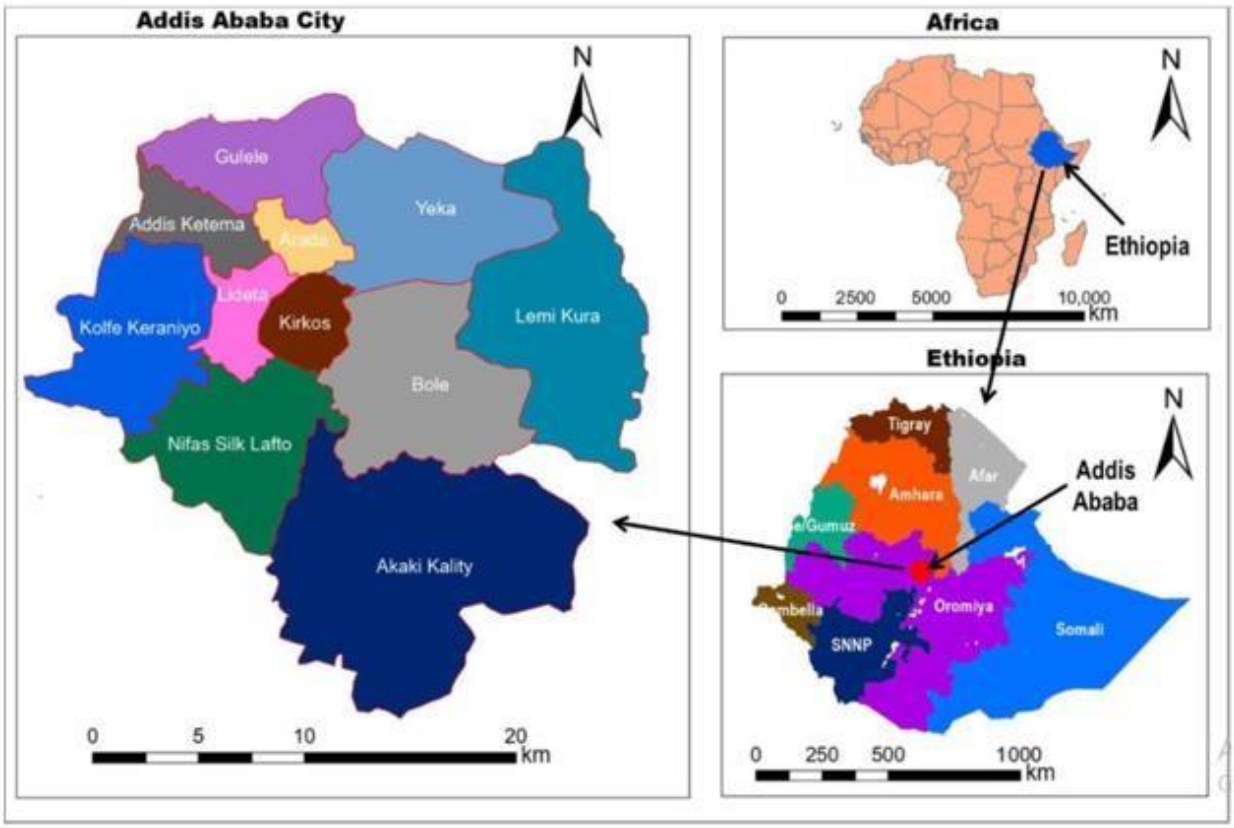

Figure 1 Addis Ababa city map

3.2. Data Description and collection

The historical daily rainfall data collected from the National Meteorological Service Agency of Ethiopia was used for the analysis of the IDF curve in Addis Ababa.

There are about 11 meteorological stations in the city. However, the author selected four stations that are Intoto, Akaki, Bole, and Observatory stations because of relatively better data availability and spatial locations.

The rest of the stations are mostly class IV (collect only rainfall) and class III (collect rainfall and air temperature), and they have been established in recent years so that they have recorded data for less than 10 years.

Table 1:- Description of Selected Stations

No	Station NAME	Latitude, Degree	Longitude, Degree	Elevation M(amsl)	Class	year of records
1	AA Bole	8.98	38.80	2330	1	1992-2021
2	AA OBS	9.02	38.75	2386	1	1992-2021
3	Akaki	8.87	38.79	2057	1	1992-2021
4	Intoto	9.08	38.73	2903	1	1992-2021

3.2.1. Climate model data sets

Coordinated Regional Climate Downscaling Experiment (CORDEX) data were used for future climate projection. CORDEX is an international effort supported by the World Climate Research Program (WRCP), aimed at producing a set of climate change projections covering different regions of the world with multiple RCMs and several emission scenarios. These regional climate projections were based on (CMIP5) projects. There are about 10 RCM participated over African domain. For this study, dynamically downscaled outputs by the recent version of the Rossby Centre Regional Climate Model—RCM 8.5 were used. The model was developed in Swidish Meteorological and Hydrological institute (SMHI). Spatially, the RCA4 simulations cover the CORDEX-Africa domain at resolution of 0.44° × 0.44° (~50 km × 50 km) for the 2010–2099 time period. It is a fine scale (approximately 50 km × 50 km) climate projection readily available to users in a grid format. In this study the bias-corrected CORDEX precipitation data developed by Liersch et al (2018) was used[1].

[1] Can be downloaded from https://dataservices.gfz-potsdam.de/pik/showshort.php?id=escidoc:3124935&show_gcmdcitation=false

3.3. Data pre- processing

3.3.1. Filling missing data

The historic record missing needs to be estimated. For this study, the inverse distance weighting method was used for the interpolation of rainfall data. This method is widely used and recommended by the United States Army Corps of Engineers (USACE, 2000).

Inverse Distance Weighting (IDW) interpolation determines cell values using a weighted combination of a set of sample points. The weight is a function of the inverse distance, which is inversely proportional to the distance between the observations and the interpolated location. This method was chosen over the other methods because it takes into account the distance of neighboring stations to the target station. Inverse weight distance was employed to determine the spatial pattern of rainfall at different time scales. The formula for estimating the missing value of an observation, PA, using the observed values at other reference stations is given by:

$$PA = \frac{\sum_{i=1}^{N} \frac{Pi}{Di_K}}{\sum_{i=1}^{N} \frac{1}{Di^K}} \quad \ldots\ldots\ldots\ldots\ldots\ldots .3.1$$

Where PA is the observation at the base station A, N is the number of neighboring stations, Pi is the observation at station i, Di is the distance from the location of station i to station A, and k is referred to as the friction distance that ranges from 1–6, and the common value 2 (Vieux, 2001) was taken for this study. The distance between stations can be estimated from their geographical location using the following expression:

$$Di^2 = (X - Xi)^2 + (Y - Yi)^2 \ldots\ldots\ldots\ldots\ldots\ldots .3.2$$

Where X and Y are the coordinates of the station whose data is estimated and Xi and Yi are the coordinates of stations whose data are used in estimation.

3.3.2. Areal mean precipitations

Thiessen polygon method

This method attempts to allow for a non-uniform distribution of gauges by providing a weighting factor for each gauge. The stations are plotted on a base map and are connected by straight lines. Perpendicular bisectors are drawn to the straight lines, joining adjacent stations to form polygons, known as Thiessen polygons (H.M. Raghunath, 2006). Areal mean precipitations were also determined from these representative stations by using the already-extracted annual maximum rainfall for each station. The Thiessen polygon mean method was adopted for the mean area (basinwide) rainfall determination as long as the method gives some weightage factor to various stations based on a rational basis. Further, the method could provide a chance for rain gauge stations outside the catchment. The IDF curve for this representative mean annual rainfall for the study area was also developed. The average depth of rainfall for the entire city is given by:

$$\bar{P} = \frac{\sum_{i=1}^{M} P^i A^i}{ATAT} = \sum_{i=1}^{M} P_i \frac{A^i}{} \quad \ldots\ldots\ldots\ldots\ldots\ldots\ldots 3.3$$

Where, $AT\ is\ total\ area\ and$ Areal ratio $\frac{A_i}{AT}$ is called the weightage factor for each station.

3.3.3. Testing for Outliers

An outlier is an observation that deviates significantly from the bulk of the data, which may be due to errors in data collection or recording or to natural causes. The presence of outliers in the data causes difficulties when fitting a distribution to the data. Low and high outliers are both possible and have different effects on the analysis. (Rao and Hamed, 2000)

The retention or deletion of these outliers can significantly affect the magnitude of statistical parameters computed from the data, especially for small samples. As it is cited in Rao and Hamed (2000), the Grubbs and Beck (1972) test is used to detect outliers. In this test, the quantities XH and XL are calculated using the following equations:

$$X_H = exp(x + K_n * S) \quad \ldots\ldots\ldots\ldots\ldots 3.4$$

$$X_L = exp(x - K_n * S) \dots \dots \dots \dots \dots \dots .3.5$$

Where X and S are the mean and standard deviations of the natural logarithm of the annual rainfall peaks, respectively, and Kn is the G-B statistic tabulated for various sample sizes and at the 10% significant level by Grubbs and Beck (1972).

Sample values greater than XH are considered to be high outliers, while those less than XL are considered to be low outliers.

3.3.4. Test for Independence and Stationery(W-W)

Given a sample of size N, the Wald-Wolfowitz (1943) (W-W) test is used to test for the independence of a data set and to test for the existence of trends in it. For a data set x1, x2, ...xn, the statistic R is calculated from Eq.

$$R = \sum_{i=1}^{n-1} X_i X_i + X_1 X_n \dots \dots \dots \dots \dots .3.6$$

When the elements of the sample are independent, R follows a normal distribution with mean and variance given by:

$$\bar{R} = (S_{12} - S_2) \dots \dots \dots \dots \dots .3.7$$

$$Var(R) = \frac{S^2}{n-1} - S^4 - \bar{R}^2 + \frac{S^1}{(N-1)(N-2)} - 4S^1 S^2 + 4S^1 S^3 + S^2 - 2S^4 \dots \dots \dots \dots \dots .3.8$$

3.3.5. Test for Homogeneity and Stationery (M-W)

In this test, two samples of size p and q with $p \leq q$ are compared. The combined data set of size $N=p+q$ is ranked in increasing order. The Mann-Whitney (M-W) test considers the quantities V and W in the equations below.

$$V = R - \frac{(P(P+1))}{2} \dots \dots \dots \dots \dots \dots .3.9$$

$$W = pq - V \ldots\ldots\ldots\ldots\ldots\ldots .3.10$$

R is the sum of the ranks of the elements of the first sample (size p) in the combined series (size N), and V and W are calculated from R, p, and q. V represents the number of times an item in sample 1 follows an item in sample 2 in the ranking. Similarly, W can be computed for sample 2 following sample 1.

The M-W statistic U is defined by the smaller of V and W. When N > 20 and p and q > 3, and under the null hypothesis that the two samples came from the same population, U is approximately normally distributed with a mean $U = \frac{pq}{2}$ and variance var (U),

$$var(U) = \left[\frac{pq}{N(N-1)}\right]\left[\frac{N^3 - N}{12} - \sum T\right] \ldots\ldots\ldots\ldots\ldots .3.11$$

Where $T = \frac{(J^3 - J)}{12}$ and J is the number of observations tied at a given rank. T is summed over all

groups of tied observation in both samples of size p and q.

The statistic $u = \frac{[U - U)]}{var(U)^{1/2}}$ is used to test the hypothesis of homogeneity at significance level □ by comparing it with the standard normal variant for that significance level (Rao and Hamed, 2000).

3.3.6. Test for Trend

In the Mann-Kendall nonparametric trend test, data values are evaluated as an ordered time series. Each data value is compared to all subsequent data values. The initial value of the Mann-Kendall statistic, S, is assumed to be 0 (no trend). If a data value from a later period is higher than a data value from an earlier period, S, is incremented by 1. On the other hand, if the data value from a later period is lower than a data value sampled earlier, S is decremented by 1. This test was chosen over other trend detection tests due to: 1) The Mann-Kendall test is a rank-based, non-parametric test. When compared to parametric tests like the t-test, the Mann-Kendall test has a higher power for non-normally distributed data, which are frequently encountered in hydrological records like precipitation .2) It has low sensitivity to abrupt breaks due to inhomogeneous time series and 3) The Mann-Kendall test has been extensively used to determine trends in similar hydrologic studies done in the past (Onoz and Bayazit, 2003). The Mann-Kendall statistic defined by variable S was

computed, which is the sum of the difference between the data points for a series (x1, x2,... xn). The S statistic, which comes from a population where the random variables are independent and identically distributed, is given by:

$$S = \sum_{i=1}^{N-1} \sum_{j=i+1}^{N} Sign(Xj - Xi) \; where \; ; Sign(Xj - Xi) = \begin{cases} +1 \; if \; (Xj - Xi) > 0 \\ 0 \; if \; (Xj - Xi) = 0 \\ -1 \; if \; (Xj - Xi) < 0 \end{cases} \ldots\ldots\ldots\ldots\ldots 3.12$$

Where S is Mann-Kendal's test statistics, Xi and Xj are maximum rainfall values of years i and j (j > i), and N is the length of the time series. A positive or negative value of S indicates an upward or downward trend (Drapela & Drapelova, 2011).

3.3.7. Testing the goodness of fit of data

For each probability distribution (EVI, lognormal, and log Pearson III), the chi-square goodness of fit test (equation 3.16) was used to see whether the data fit the theoretical frequency distributions for annual maximum rainfall values of all durations and stations under consideration.

Probability distribution fitting was carried out just to define which particular distributions would automatically fit a given set of data series. The areal annual maximum daily data series were extracted for the four stations and fitted to the most commonly used distribution functions, namely, the Gumbel, Log-Pearson type III, and Log normal distributions. The reliability of the best-fit probability distribution function was made based on goodness-of-fit (GOF) test criteria in terms of Kolmogorov-Smirnov (K-S), Anderson-Darling (A-D), and Chi-square criteria. This way of selecting fitting probability distributions was adopted because the fitting process relies on computations of fitness parameters based on sample data. This would assist in ranking the fitted distributions according to the quality of fit over the raw data. GOF tests measure the compatibility of a random sample with a theoretical probability distribution function.

Kolmogorov-Smirnov (K-S) Test

This test is used to decide if a sample comes from a hypothesized continuous distribution. It is based on the empirical cumulative distribution function (ECDF). Assume that we have a random sample $X1,\ldots, Xn$ from some distribution with CDF $F(x)$. The empirical CDF is denoted by:

$$F_n(X) = \frac{1}{n}[number\ of\ observations \leq x] \ldots\ldots\ldots\ldots\ldots .3.13$$

The Kolmogorov-Smirnov statistic (D) is based on the largest vertical difference between the theoretical and the empirical cumulative distribution function:

$$D = \max_{1 \leq i \leq n}\left(F(x_i) - \frac{i-1}{n}, \frac{1}{n} - F(x_i)\right) \ldots\ldots\ldots\ldots\ldots .3.14$$

Chi-Squared Test

The chi-squared test is used to determine if a sample comes from a population with a specific distribution. This test is applied to binned data, so the value of the test statistic depends on how the data is binned.

The data can be grouped into intervals of equal probability or width. Each bin should contain at least five or more data points, so certain adjacent bins sometimes need to be joined together for this condition to be satisfied. Although there is no optimal choice for the number of bins (k), there are several formulas that can be used to calculate this number based on the sample size (N).

$$K = 1 + \log_2 N \ldots\ldots\ldots\ldots\ldots .3.15$$

the chi-squared statistic is defined as; $x^2 = \sum_{i=1}^{K} \frac{(O_i - E_i)^2}{E_i} \ldots\ldots\ldots\ldots\ldots .3.16$

Where O_i is the observed frequency for bin i and E_i is the expected frequency for bin i calculated by; $E_i = F(x_2) - F(x_1)$

Where F is the CDF of the probability distribution being tested, and x1, x2 are the limits for bin i.

Anderson-Darling Test

The Anderson-Darling procedure is a general test to compare the fit of an observed cumulative distribution function to an expected cumulative distribution function. This test gives more weight to the tails than the Kolmogorov-Smirnov test. The Anderson-Darling statistic (A2) is defined as:

n

$$A^2 = -n - \frac{1}{n}\sum_{i=1}(2i-1) * \left[\ln\left(1 - F(x_{n-i+1})\right)\right] \quad \ldots\ldots\ldots\ldots\ldots\ldots .3.17$$

The fitting of observed data with respect to the best selected fitting function was presented as a quantile-quantile (Q-Q) plot, which is a graph of the input (observed) data values plotted against the theoretical (fitted) distribution quantiles. Both axes of this graph are in units of the input data set (i.e., millimeters). The Q-Q plot helps to judge, by visual inspection, which types of distribution functions were appropriately fitted to the data.

$$F^{-1}(F_n(x_i) - 0.5 \quad \ldots\ldots\ldots\ldots\ldots\ldots .3.18 \qquad \frac{}{n}$$

Where: F^{-1} - inverse cumulative distribution function (ICDF)

F_n ---- Empirical CDF; n ----- Sample size

3.4. Rainfall Intensity Duration Frequency Analysis

Computation of extreme value (XT)

Calculating the magnitudes of extreme events by the probability distribution function method is recommended for those that are invertible. Calculating the magnitudes of extreme events requires that the probability distribution function be invertible; that is, given a value for *T,* the corresponding value of XT can be determined. Some probability distribution functions are not readily invertible, including the Normal and Pearson Type III distributions, and an alternative method of calculating the magnitudes of extreme events is required for these distributions (Chow et al., 1987). The magnitude XT of a hydrologic event may be represented as the mean plus the departure of the variate from the mean.

$$X_T = \bar{X} + \Delta X_T \ldots\ldots\ldots\ldots 3.19$$

The departure may be taken as equal to the product of the standard deviation and a *frequency factor KT; that* is, the departure and the frequency factor *KT* are functions of the return period and the type of probability distribution to be used in the analysis. Therefore, it can be expressed as

$$X_T = \bar{X} + \delta K_T \ldots\ldots\ldots\ldots\ldots .3.20$$

$$\delta = \ldots\ldots\ldots\ldots\ldots\ldots\ldots 3.21 \quad \sqrt{\frac{\sum(x-\bar{x})^2}{N-1}}$$

$$\bar{X} = \sum_{i=1}^{n} X_i \ldots\ldots\ldots\ldots\ldots\ldots\ldots 3.22 \quad \frac{\sum X}{n}$$

For the Extreme Value Type I distribution, (Chow, 1953) derived the expression for frequency factor KT:

$$K_T = -\frac{\sqrt{6}}{\pi}\left\{0.5772 + \ln\left[\ln\left(\frac{T}{T-1}\right)\right]\right\} \ldots\ldots\ldots\ldots\ldots 3.23$$

Log-Pearson Type III Distribution: For this distribution, the first step is to take the logarithms of the hydrologic data, y = log *x*. Usually, logarithms to base 10 are used. The mean, standard deviation, and coefficient of skewness Cs are calculated for the logarithms of the data. The frequency factor depends on the return period *T* and the coefficient of skewness Cs. When Cs ≠ 0, *KT* is approximated by

$$3.24\ K_T = z + (z^2 - 1)k + \frac{1}{3}(z^3 - 6z)k^2 - (z^2 - 1)k^3 + zk^4 + \frac{1}{3}k^5 \ldots\ldots\ldots\ldots\ldots$$

$$where\ ;\ k = \frac{C_s}{6}$$

$$C_s = \frac{\sum_{i=1}^{n}(Y_i - \bar{Y})^3}{(n-1)(n-2)\delta_y^3} \ldots\ldots\ldots\ldots\ldots\ldots 3.25$$

For Log-normal distribution, the mean *Y;* standard deviation δ; and coefficient of skewness Cs are calculated for the logarithms of the data and for a case, Cs, the frequency factor is equal to the standard normal variable z.

$$K_T = Z = \frac{X_T - \bar{X}}{\delta} \quad FOR\ normal\ distribution \ldots\ldots\ldots 3.26$$

For log normal distribution, the following formula can be used for determining the frequency factor (KT=Z);

$$K_T = z = w - \frac{(2.516 + 0.8028w + 0.0103w^2)}{[(1 + 1.4328w + 0.1893w^2 + 0.0013w^3)]} \ldots\ldots\ldots\ldots\ldots..3.27$$

where w is intermediate variable and p is probability of exceedance; w will be calculated using the following formula:

$$w = [\ln (P_{-2})]^{1/2} \qquad (0 < P \leq 0.5) \ldots\ldots\ldots..3.28$$

For the lognormal distribution, the Log Pearson Type III procedure is applied except for the frequency factor KT=Z; for Cs =0, that is applied to the logarithm of the variables.

After identifying the best fit type of probability distribution for a given annual maximum observed data, the extreme rainfall events (XT) were calculated for a return period of 2, 5, 10, 25, 50, and 100 years.

Calculating Intensity of Rainfall (*i*)

For a given calculated extreme rainfall depth for a given return period, the corresponding intensity of rainfall was computed by:

$$i = \frac{R}{d}$$

where R is rainfall depth in mm and d is duration in hr. However, the raw data collected from ENMA was based on a daily base time series. In order to get a fine-resolution time series of data in minutes for analysis, annual maximum daily data were disaggregated into the required d time series (10, 20, 30, 40, 50, up to 180 minutes) by using the relation recommended by the ERA 2013 drainage design manual.

$$RR_t = \left(\frac{t}{24}\right)\left[\left(\frac{b + 24}{b + t}\right)^n\right] \ldots\ldots\ldots\ldots\ldots\ldots.3.29$$

Where RR_t = rainfall ratio; R_t: R_{24}

R_t= rainfall in a given duration t in hours R_{24} = rainfall in 24 hours

t= time in hours, based on the studies of a large number of gauges in east Africa, (ERA 2013), b =0. 3, n= 0.94($0.78 \leq n \leq 1.09$)

3.5. Comparison of IDF Results

IDF curves for respective future climate change scenarios were compared with the present IDF curves of the respective stations. The relative difference (RD) between the curves was determined using the following relationship given by Solaiman and Simonovic (2010):

$$RD = \frac{(X1 - X2)}{\left(\frac{X1 + X2}{2}\right)} * 100 \quad \ldots\ldots\ldots\ldots\ldots\ldots .3.30$$

Where X1 is the intensity of rainfall under future climate change (mm/hr), X2 is the intensity of rainfall under the present climate condition (mm/hr). The purpose of the comparison of these results was to assess whether the rainfall intensity will increase or decrease under climate change for all durations and return periods of the respective stations (Simonovic and Peck, 2010).

Software Packages Used

Microsoft Excel 2021: Used for Data Management and IDF Plotting

ArcGIS 10.7.1: Used for study area delineation and to calculate average area rainfall using the Thiessen polygon.

Easy Fit computer program is used to test the goodness of fit of probability distribution functions.

4.RESULTS AND DISCUSSIONS

4.1. filling missing value of rainfall data

Rainfall data gap filling was done by IDW method using Microsoft Excel. The number of days with filled data at AA Bole, AA Observatory, Akaki and Intoto stations, respectively, were 725, 90, 54 and 31 days.

4.2. Areal mean precipitations

To calculate the 1992 year of maximum annual daily rainfall data of all the stations selected for the analysis of the average area rainfall for Addis Ababa city using the Thiessen polygon method, the result from ArcGIS is that the summation of percent of the average depth of rainfall is the rest of the year, from 1993 to 2021, is analyzed in this way and is given in Appendix Tables. *Table 2 Areal rainfall for 1992 year*

No	Station NAME	Elevation m (amsl)	Longitude	Latitude	Rainfall mm	AREA(Sq.m	percent
1	AKAKI	2057	38.79	8.87	38.2	113	8.28
2	AA BOLE	2330	38.80	8.98	44.3	210	17.85
3	AA OBS	2386	38.75	8.87	51.4	152	15.00
4	INTOTO	2903	38.73	9.08	43.7	46	3.85

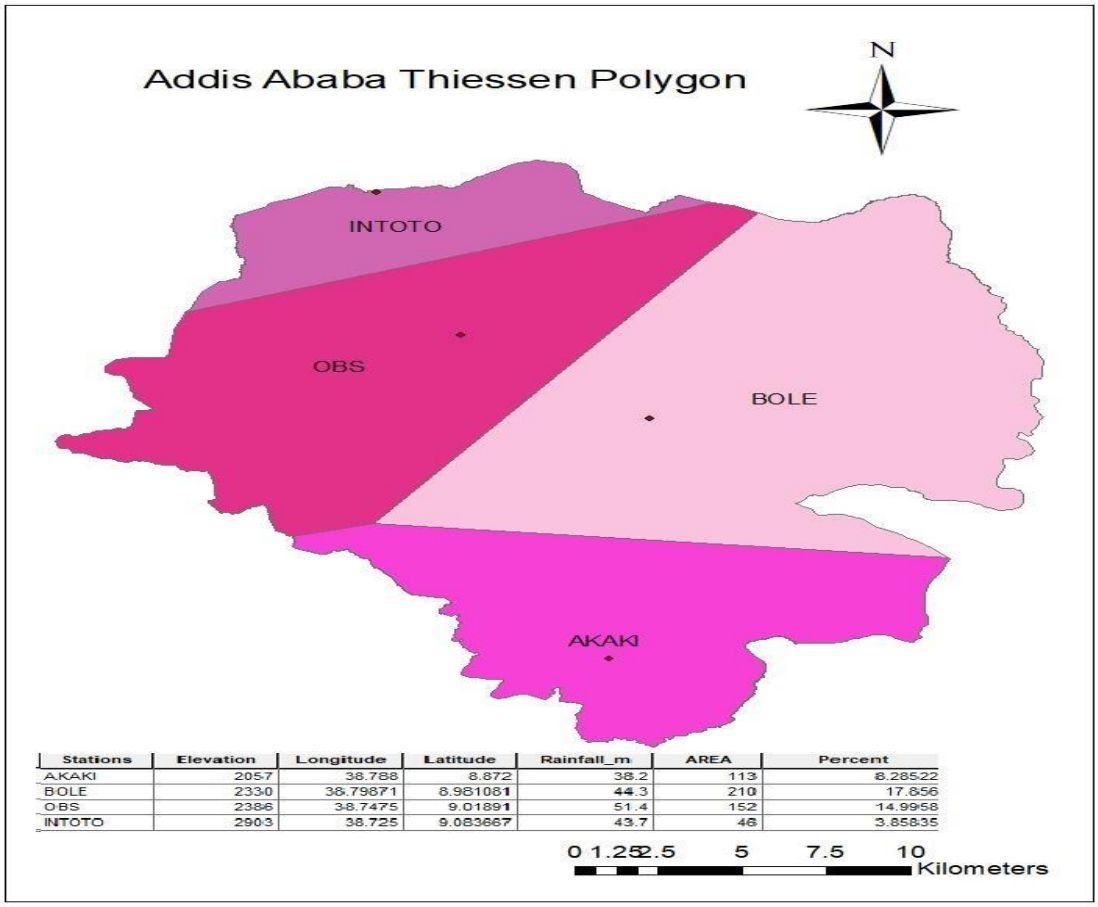

Stations	Elevation	Longitude	Latitude	Rainfall_m	AREA	Percent
AKAKI	2057	38.788	8.872	38.2	113	8.28522
BOLE	2330	38.79871	8.981081	44.3	210	17.856
OBS	2386	38.7475	9.01891	51.4	152	14.9958
INTOTO	2903	38.725	9.083667	43.7	46	3.85835

Figure 2 :- Thiessen polygon for Addis Ababa

The total rainfall of 30 years of data for Addis Ababa city is summarized below. By using this data, a quality check was performed and an IDF curve was formulated.

year	max daily annual rainfall(mm)	Year	max annual rainfall
1992	45.00	2007	59.65
1993	49.55	2008	44.42
1994	48.10	2009	54.95
1995	64.67	2010	60.43
1996	54.07	2011	51.24
1997	53.10	2012	47.92
1998	62.76	2013	41.44

1999	41.78	2014	41.33
2000	43.07	2015	50.11
2001	55.38	2016	42.68
2002	32.54	2017	48.88
2003	46.52	2018	43.37
2004	36.68	2019	49.64
2005	47.90	2020	114.19
2006	61.93	2021	44.95

Table 3:- Maximum Annual rainfall for historic record

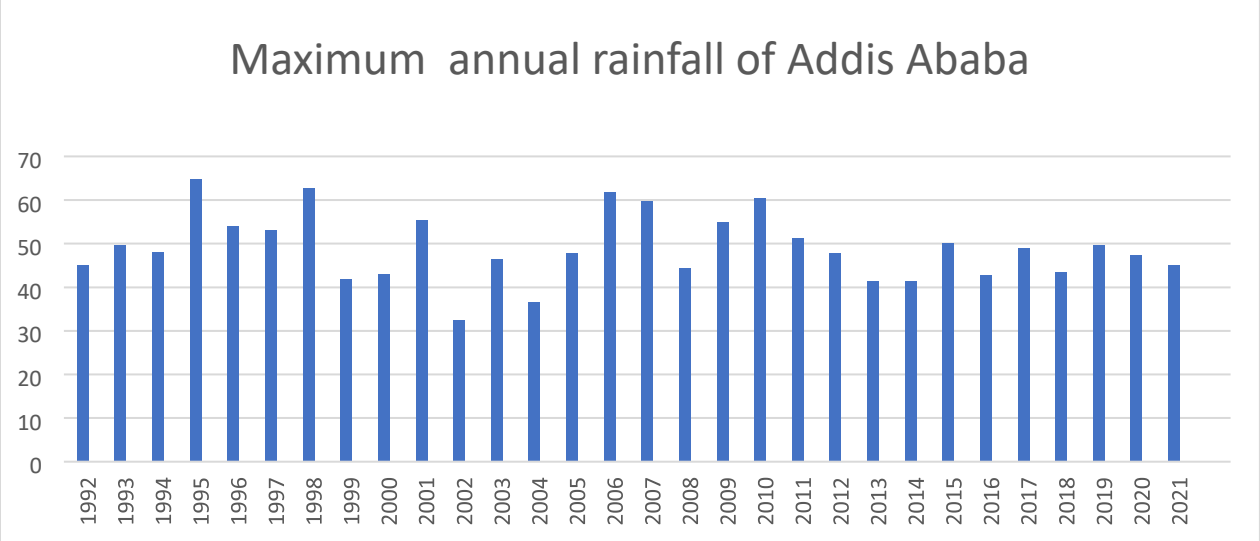

Figure 3:- Addis Ababa Maximum annual rainfall for historic record

4.3. Tests for Maximum Annual daily rainfall data

4.3.1. Test for Outliers

Using the G-B test, we can determine the lower and upper outlier limits for historic rainfall, as the mean is X = 3.88074, and the standard deviation is *s* = 0.158998. The *Kn value* can be K_N = G-B statistics at 10% significance level, as approximated by Pilonet et al. = K_N =2.563, where N = 30. After this, it is quite possible to calculate the upper and low outliers. The upper outlier limit is about XH = 72.83871, and the lower outlier limit is XL = 32.24054.

Therefore, from the above analysis of the outliers (upper or lower) for observed year data, there is no single data that falls under the range of the outliers, as we can observe from the maximum daily annual rainfall data presented above, Hence, there is no annual maximum daily data with outliers.

4.3.2. Test for Homogeneity and Stationarity

Using the Mann-Whitney (1947) (M-W) test for observed rainfall data, we can determine the parameters for the test as shown below. The first step in the calculations of homogeneity and stationery is to subdivide the data into p and q data series with p = 15 and q = 15.

J is the number of observations of an element tied at a given rank. We can rank the combined data set series in the increasing order described above. Following this, it is possible to determine R, V, W, and U as follows: R is the sum of the ranks of the elements of the first sample (size p) in the combined series (size N).

$$R = 11 + 18 + 16 + 30 + 23 + 22 + 29 + 5 + 7 + 25 + 1 + 12 + 2 + 14 + 28$$

$$R = 243$$

we can determine the values of V and W, as follows.

$$V = R - \frac{\left(P(P+1)\right)}{2}$$

$$V = 243 - \frac{\left(15(15+1)\right)}{2}$$

$$V = 123$$

Again, W can also be determined from the above formula. $W = Pq - V$, $W = 102$

Accordingly, we can also determine U from the approaches given above. In the concept above, U is the smaller value of V and W. This leads to that. U =102

In the same fashion, we can also determine and var(U) accordingly.

$$U = \frac{pq}{2}$$

$$U = \frac{15 * 15}{2}$$

$$U = 112.5$$

$$\underset{var}{(U)} = \left[\frac{pq}{N(N-1)}\right]\left[\frac{N^3 - N}{12} - \sum_{T]}\right]$$

The summation of T is zero as there are no *J* values observed as tied observations at a given rank.

$$\underset{var}{(U)} = \left[\frac{15 * 15}{30(30-1)}\right]\left[\frac{30^3 - 30}{12} - 0\right]$$

This guide us to: $var(U) = 581.25$ As a result, it is possible to determine the statistic u from the formula below.

$$u = \frac{(U - \bar{U})}{[var(U)]^{1/2}}$$

$$u = \frac{(102 - 112.5)}{[581.25]^{1/2}}$$

$$u = -0.43552$$

Since $|u| = 0.435552$, is less than the critical value $U_{0.025} = 1.96$, the study area with a maximum annual daily rainfall data can be considered to be homogeneous and stationary at the 5% level of significance, means that the data comes from the same distribution and seasonal. **Climate scenario RCP 8.5 Homogeneity and Stationary Test**

the analysis of the homogeneous and stationary for climate RCP 8.5 (2010-2039) results, $|u| = 0.145173$, is less than the critical value $U_{0.025} = 1.96$, the study area with an average annual daily rainfall data can be considered to be homogeneous and stationary at the 5% level of significance.

Therefore, from the above analysis of the homogeneous and stationary results observed and the climate scenario RCP 8.5 from (2010-2039), (2040-2069), and (2070-2099) years, the projected rainfall data can be considered to be homogeneous and stationary at the 5% level of significance. The RCP 8.5 (2010-2039); (2040-2069) and (2070-2099) year climate scenario data of homogeneous and stationary results are presented under the annex table 9.

4.3.3. Test for Independence and Stationarity

Using the Wald-Wolfowitz (1943) (W-W) test, the study area of historic rainfall data maximum annual daily rainfall data can be calculated and the values determined. Hence, it follows as below:

The statistic R can be calculated as below like.

$$n-1$$

$$R = \sum_{i=1} X_i X_{j+1} + X_1 X_n \ldots$$

$$R = 44.99537 * 49.55413 + 49.55413 * 48.09501 + \cdots.$$

$$R = 72411.04$$

Accordingly, R follows the mean and variance of the following values.

$$R = \frac{(S^{12} - S^2)}{N - 1} \ldots \ldots \ldots$$

As mentioned above, the values of $s_r = Nm_r$, where m_r is the r[th] moment of the sample about the origin

$$Var(R) = \frac{S^2}{n-1} - S_4 - \bar{R}^2 + S\frac{}{(N-1)(N-2)} 14 - 4S_{12}S_2 + 4S_1S_3 + S_{22} - 2S_4 \ldots \ldots \ldots \ldots$$

Hence the sample moments about the origin, which implies α=0, Xi=0= raw score.

First moment $(M_1) = \frac{1}{N}\sum_{i=1}^{N} X_I$

Second Moment(M_2) $(M_2) = \frac{1}{N}\sum_{i=1}^{N} X_i^2$

Third Moment (M_3) $(M_3) = \frac{1}{N}\sum_{i=1}^{N} X_i^3$

Forth Moment (M_4) $(M_4) = \frac{1}{N}\sum_{i=1}^{N} X_i^4$

From this table $S_1 = 1471.504$ $S_2 = 73911.99$

$S_3 = 37988110$ $S_4 = 199599072.6$

Accordingly, R follows the mean and variance of the following values.

$$R = \frac{(S^{12} - S^2)}{} \ldots \ldots \ldots$$

$$N - 1$$

$$\bar{R} = \frac{(1471.504^2 - 73911.99)}{30 - 1}$$

$$\bar{R} = 72117.62$$

$$Var(R) = \frac{S_{22} - S_4 - \bar{\bar{2}}}{n-1} + \frac{S_{14} - 4S_{12}S_2 + 4S_1S_3 + S_{22} - 2S_4}{(N-1)(N-2)} R$$

Inserting the values to the equation and the result will be

$$Var(R) = \frac{73911.99^2 - 199599072.6}{31 - 1} - \overline{72117.62^2} + \frac{1471.504^4 - 4 * 1471.504^2 * 73911.99 + 4 * 1471.504 * 37988110 + 73911.99^2 - 2 * 199599072.6}{(30-1)(30-2)}$$

$$Var(R) = \quad 93972.58$$

$$u = \frac{(R - \bar{R})}{[var(U)]^{1/2}}$$

$$u = \frac{(72411.04 - 72117.62\ )}{[93972.58]^{1/2}}$$

$$u = 0.957185$$

Conclusion The test value is less than the critical value at the 5% significance level ($U_{0.025} = 1.96$). Thus, we can accept the hypothesis of independence and stationarity. The study area of average annual daily rainfall data is concluded to be independent and stationary at the 5% significance level.

Climate scenario RCP 8.5 Independence and Stationarity test

Using the Test for Independence and Stationarity test, the climate scenario RCP 8.5 (2010–2039year data) of Addis Ababa city's annual maximum daily rainfall data can be calculated, and the values can be determined in the same step as the observed rainfall data is checked. Hence, it follows as below: The analysis of RCP 8.5(2010-2039); (2040-2069) and (2070-2099) is presented in the Annex Table10-17.

Conclusion The test value is 0.56146909 less than the critical value at the 5% significance level ($U_{0.025} = 1.96$). Thus, we can accept the hypothesis of independence and stationarity. The study area of average annual daily rainfall data is concluded to be independent and stationary at the 5% significance level.

Therefore, from the above analysis of the independent and stationary for observed and the climate scenario RCP 8.5 from (2010-2039); (2040-2069), and (2070-2099) years, the projected rainfall data can be considered independent and stationary at 5% level of significance.

4.3.4. Test for trend

In the Mann-Kendall nonparametric trend test, data values are evaluated as an ordered time series. Each data value is compared to all subsequent data values.

The formula below is used for the analysis of Mann-Kendal's test statistics(S). We can rank the combined data set series in the increasing order described above. Following this, it is possible to determine S and Var (s) as follows:

$$S = \sum_{i=1}^{N-1} \sum_{j=i+1}^{N} Sign(Xj - Xi) \; where \; ; Sign(Xj - Xi) = \begin{cases} +1 \; if \; (Xj - Xi) > 0 \\ 0 \; if \; (Xj - Xi) = 0 \\ -1 \; if \; (Xj - Xi) < 0 \end{cases}$$

Where S is Mann-Kendal's test statistics, Xi and Xj are maximum rainfall values of years i & j (j > i),

$$S = -91$$

$$var\ s = \frac{N(N-1) * 2N + 5}{18}$$

$$var\ s = 3141.667$$

$$Z\ Statstic = \left| \frac{S}{\sqrt{(var\ s)^2}\, Z} \right|$$

$$Statstic = 1.623534$$

Conclusion: The test value is less than the critical value at the 5% significance level ($U_{0.025}$ = 1.96). Thus, we can accept the hypothesis of Mann-Kendal's trend test. The study area of historic maximum annual daily rainfall data is concluded to have **no trend at the 5% significance level.**

Climate scenario RCP 8.5 Trend Test

Mann-Kendall nonparametric trend test: climate projected RCP8.5 2010–2039-year rainfall data values are evaluated as an ordered time series. Each data value is compared to all subsequent data values.

Conclusion: The test value is less than the critical value at the 5% significance level ($U_{0.025}$ = 1.96). Thus, we can accept the hypothesis of Mann-Kendal's trend test. The Study Maximum annual daily rainfall data are concluded to show no trend at the 5% significance level.

Therefore, from the above analysis of the trend test for observed and the climate scenario RCP 8.5 from 2010–2039, 2040–2069, and 2070–2099, the projected rainfall data can also be considered; there is no trend at the 5% significance level. RCP 8.5(2010-2039); (2040-2069) and (2070-2099) year climate scenario data of trend test results are presented under the annex table 18-21.

4.4 Selection of best fit Probability Distribution Functions

Probability distributions are used in the frequency analysis of hydrologic and meteorological data to connect the frequency and size of extreme events. All required distributions for easy-fit software were taken into account in this study, and comparisons were based on how well the test result matched expectations.

The best-fit probability density function could be identified due to the Easy Fit software. According to the criteria that the distribution with the highest overall score is chosen as the best distribution type, first, second, and third, respectively, test scores ranging from one to three (1-3) are given to each distribution type. Generally, the distribution with the highest statistic value received a score of three (3), while the next-best distributions received scores of two (2) and one (1). The person with the top rank received three (3) points, the person in second place received two (2) points, and the person in third place received one (1) point. Then, the overall rank was based on the total score earned from the Kolmogorov S. and Anderson D. Chi-squared (goodness of test) criteria. Hence, the generalized extreme value function was selected as the best probability density function that works for Addis Ababa city's maximum annual daily rainfall data. The result below shows a summary of the distribution of the easy-fit software.

	Kolmogorov Smirnov		Anderson Darling		Chi Squared	
Distribution	Statistic	Rank	Statistic	Rank	Statistic	Rank
Beta	0.11	11	0.39	10	1.62	9
Chi-Squared	0.13	13	0.69	12	3.25	13
Chi-Squared (2p)	0.07	2	0.29	4	1.21	3
Exponential	0.47	20	9.96	20	99.23	18
Exponential (2p)	0.31	17	4.96	15	11.84	15
Gamma	0.09	5	0.27	2	1.77	12
Gamma(3p)	0.09	6	0.28	3	1.74	11
Gen. Extreme Value	0.08	3	0.25	1	1.23	5
Gen. pareto	0.10	7	7.84	18	N/A	
Gumbel max	0.05	1	0.39	9	0.37	1
Laplace	0.13	15	0.58	11	1.18	2
Logistic	0.11	9	0.39	8	7.70	14
Normal	0.11	10	0.37	7	1.28	6
pareto	0.35	19	7.04	17	23.22	16
Student's t	0.97	21	218.43	21	94197.00	19

Table 4:-computed summary of the distribution of the easy-fit software for historic rainfall data

So, the software considers using all the formulae or methods of identifying the best fitting distribution function, which include Kolmogorov-Smirnov, Anderson-Darling, and Chi-Squared test methods. From these three methods, the author selects the best fit by taking the average rank of all three methods and selecting the smaller one, which is the generalized extreme value function.

Annual maximum daily rainfall data distribution fitting result

Fitting Result			
Distribution			Parameter
Generalized Extreme Value			K=-0.138
			σ=7.11
			μ=45.812

Table 5:- fitting result for historic data

The mean, variance, standard deviation, coefficient of variation, skewness, and kurtosis can also be calculated from the maximum annual daily rainfall data using easy-fit software analysis.

Descriptive statistics

sample size	30
Range	32.13
Mean	49.05
Variance	59.81
St. Deviation	7.73
Coeff Var	0.16
Skewness	0.26
Kurtosis	-0.16
min	32.54
Max	64.67

Table 6:- descriptive statistics result for historic rainfall data

Climate scenario RCP 8.5 best fit Probability Distribution Functions

So, the software considers using all the formulae or methods of identifying the best fitting distribution function, which include Kolmogorov-Smirnov, Anderson-Darling, and Chi-Squared test methods. From these three methods, the author selects the best fit by taking the average rank of all three methods and selecting the smaller one, which is the generalized extreme value function for RCP 8.5 2010-2099 Year data.

The result below shows the summary of the distribution of the easy-fit software for climate scenario RCP 8.5 (2010–2029) year rainfall data.

	Kolmogorov Smirnov		Anderson Darling		Chi Squared	
Distribution	Statistic	Rank	Statistic	Rank	Statistic	Rank
Beta	0.12	9	2.58	13	1.5	4
Chi-Squared	0.28	17	15.53	18	6.25	13
Chi-Squared (2p)	0.11	8	0.77	7	1.43	2
Exponential	0.30	18	4.62	15	22.20	16
Exponential (2p)	0.14	13	1.84	11	5.03	10
Gamma	0.09	7	0.33	6	5.40	12

Gamma(3p)	0.08	3	0.27	5	7.09	14
Gen. Extreme Value	0.07	1	0.22	1	4.14	8
Gen.pareto	0.09	6	4.11	14	N/A	
Gumbel max	0.08	4	0.27	4	5.36	11
Laplace	0.14	12	0.81	9	3.01	6
Logistic	0.12	10	0.79	8	1.45	3
Lognormal(3p)	0.07	2	0.26	3	4.19	9
Normal	0.13	11	0.94	10	1.35	1
pareto	0.22	16	4.62	16	20.93	15
Student's t	0.97	19	223.31	19	60596	17

Table 7:- computed summary of the distribution of the easy-fit software for Climate RCP8.5 rainfall data

Using easy-fit software analysis, it is also possible to calculate the mean, variance, standard deviation, coefficient of variation, skewness, and kurtosis from the values of the maximum annual daily rainfall data.

Descriptive statistics	
sample size	30
Mean	68.11
Variance	1030.5
St. Deviation	32.10
Coeff Var	0.47
Skewness	1.24
Kurtosis	1.54
Min	26.75
Max	158.94

Table 8:- descriptive statistics result for Climate RCP8.5 rainfall data

4.5. Construction of IDF curve for Historical rainfall data

The computed rainfall quantiles for specified durations and respective return periods using the historic (1992–2021) and RCP8.5 climate scenario data of 2010–2039, 2040–2069, and 2070–2099-time horizons for the city considered are summarized in Appendix Tables (22-27). while the IDF curve were illustrated below.

The table below shows Maximum annual daily rainfall data of historical data

Year	0	1	2	3	4	5	6	7	8	9
1990			45.00	49.55	48.10	64.67	54.07	53.10	62.76	41.78
2000	43.07	55.38	32.54	46.52	36.68	47.90	61.93	59.65	44.42	54.95
2010	60.43	51.24	47.92	41.44	41.33	50.11	42.68	48.88	43.37	49.64
2020	47.48	44.95								

Table 9:- Maximum Annual daily rainfall data for historical

Since the data are in daily format, we must convert them to sub-hourly time intervals utilizing ERA raw data that was gathered from NMA and was based on a daily base time series. It must be converted to a shorter length because the available rainfall depth is for a 24-hour period. Annual maximum daily data were disaggregated into the necessary d time series (10, 20, 30, 40, 50, up to 120 minutes) using the relation suggested by the ERA 2013 drainage design manual in order to obtain a fine-resolution time series of data in minutes for analysis.

$$RR_t = \left(\frac{t}{24}\right)\left[\left(\frac{b+24}{b+t}\right)^n\right]$$

Where RR_t = rainfall ratio; R_t: R_{24}

R_t= rainfall in a given duration t in hours

R_{24} = 24 hours rainfall in depth t= time in hours, based on the studies of a large number of gauges in east Africa, b =0.

3, n= 0.94(0.78≤n≤1.09)

After rearrangement, the above formula has the following form.

$$R_t = \left(\frac{t}{24}\right)\left[\left(\frac{b+24}{b+t}\right)^n * R_{24}\right]$$

After substituting intensity (I_t=R_t/t), the above formula has the following form.

$$I_t = \left(\frac{R_{24}}{24}\right)\left[\left(\frac{b+24}{b+t}\right)^n\right]$$

So, we can use the above equation to change daily rainfall to short duration rainfall

After changing this IDF curve development is implemented using generalized extreme value frequency distribution function. Using frequency factor below

$$K_T = -\frac{\sqrt{6}}{\pi}\{0.5772 + \ln[\ln(\frac{T}{T-1})]\}$$

Return Period	KT
2	-0.16
5	0.72
10	1.31
15	1.64
25	2.04
50	2.59
100	3.14

Table 10:- computed frequency factor

After calculating the frequency factor this IDF curve is developed for different return period

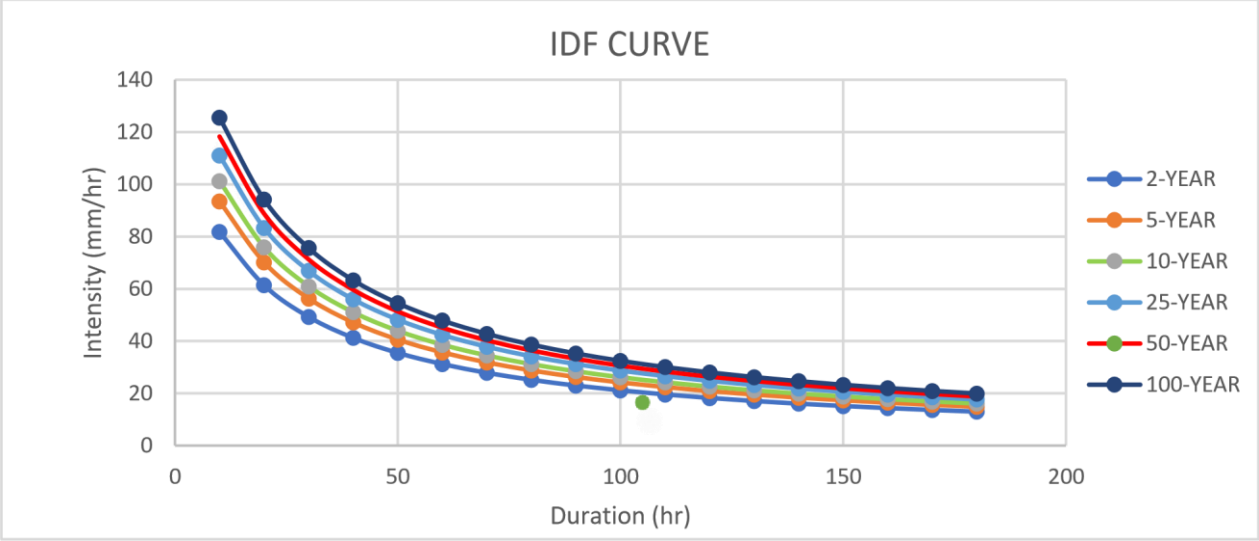

Figure 4:- Computed IDF Curve for historic rainfall data

4.6. Construction of IDF curve for Climate scenario RCP 8.5

The procedure is the same as historical data. IDF curve development is applied for climate scenario RCP 8.5. Climate scenario RCP 8.5 (2010–2039), (2040-2069) and (2070-2099) year data is illustrated below,

Maximum annual daily rainfall of climate scenario RCP 8.5 (2010-2039) year data

Year	0	1	2	3	4	5	6	7	8	9
2010	137.4	133	41.7	46.8	69.95	76.82	85.29	26.75	36.2	59.23
2020	64.45	159	56	39.7	61.09	51.67	66.43	32.85	74.1	56.89
2030	90.89	75.7	33.9	61.45	65.96	79.49	83.64	104.2	31.5	40.96

By using the above maximum daily data, we can change the daily to short duration of rainfall of climate scenario RCP 8.5 (2010-2039) with the same procedure as the historic rainfall data.

After calculating the frequency factor this IDF curve is developed for different return period

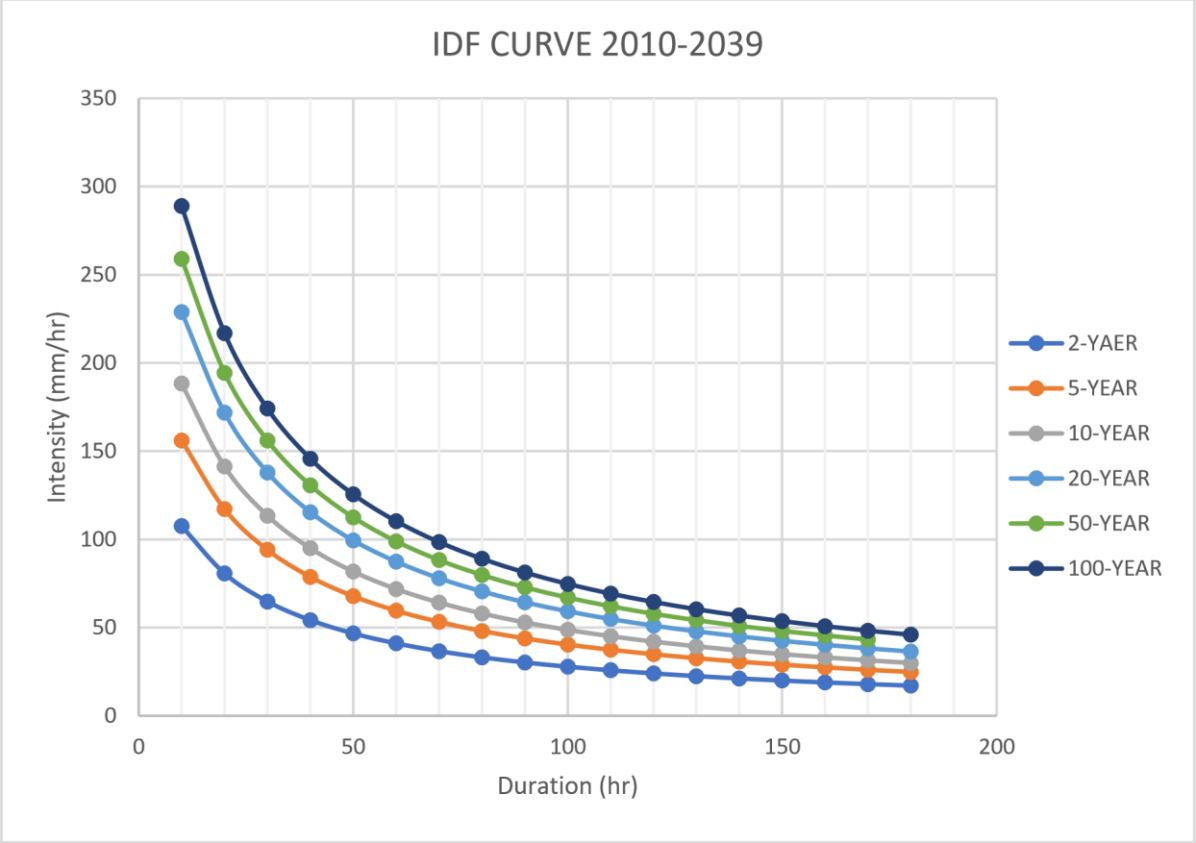

Figure 5:- IDF Curve for Climate RCP 8.5 rainfall data

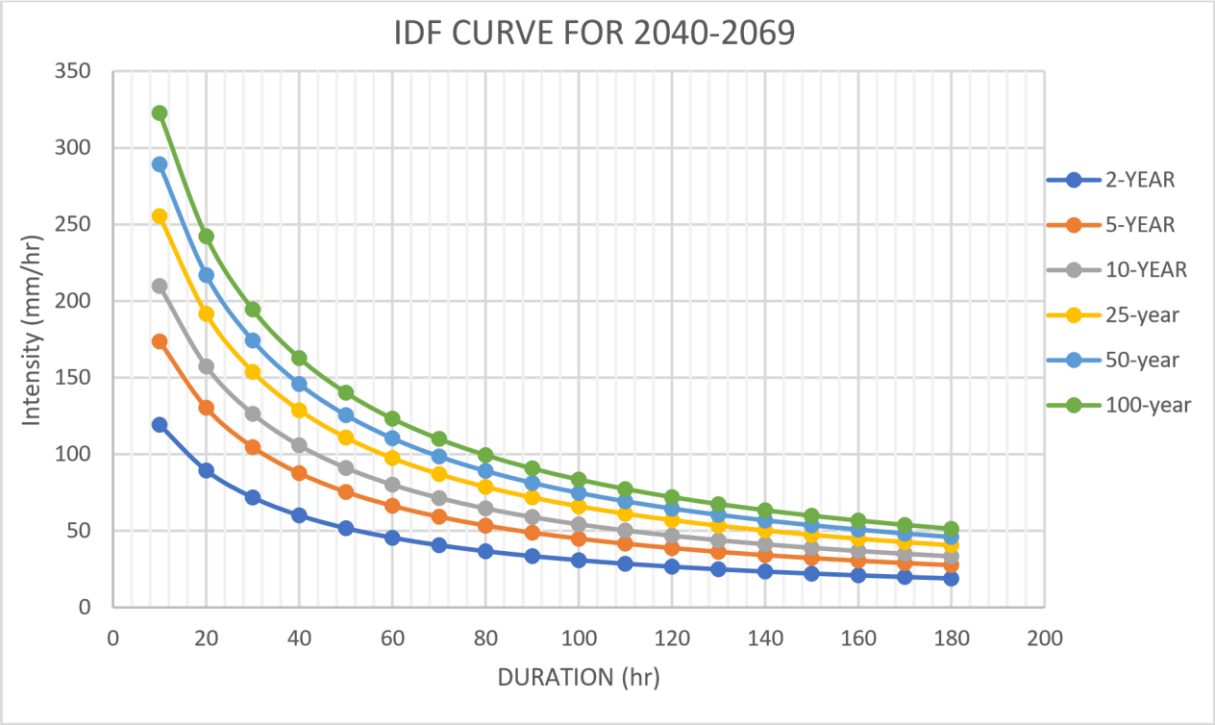

Figure 6:- IDF Curve for Climate RCP 8.5(2040-2069) rainfall data

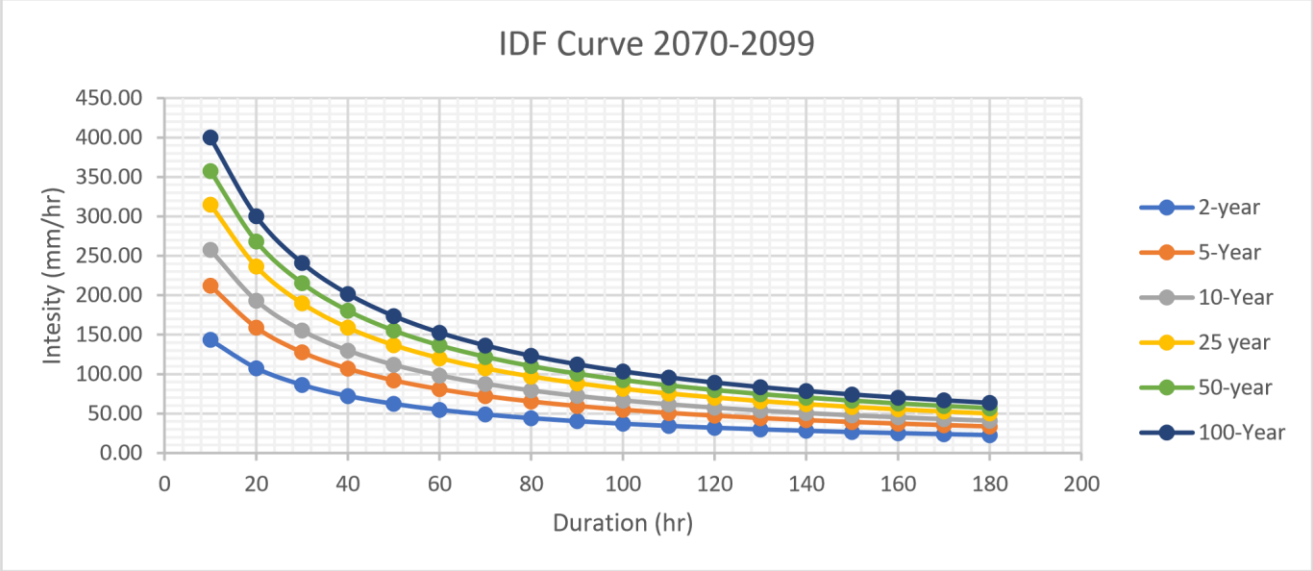

Figure 7:- IDF Curve for Climate RCP 8.5(2070-2099) rainfall data

4.7. Comparison of Current and Future IDF Results

To measure the change in rainfall intensities, IDF curves created for the city under investigation under the coming climate change scenario RCP 8.5 were compared with IDF findings from the historic climate circumstances. Using the equation 3.30, the relative difference between the present

and future curves was calculated to compare changes in rainfall intensities. The tables provide an overview of the comparison's findings.

Relative difference between historical and future climate scenario RCP 8.5						
Return period	2	5	10	25	50	100
Observed & RCP 8.5 (2010-2039)	27%	50%	60%	69%	75%	79%
Observed & RCP 8.5 (2039-2069)	37%	60%	70%	79%	84%	88%
Observed & RCP 8.5 (2070-2099)	55%	78%	87%	96%	101%	104%

Table 11:- Comparison of Current and Future IDF Results

When we evaluate the observed and the climate scenario data there is an increase of the intensity with an increase of the return period

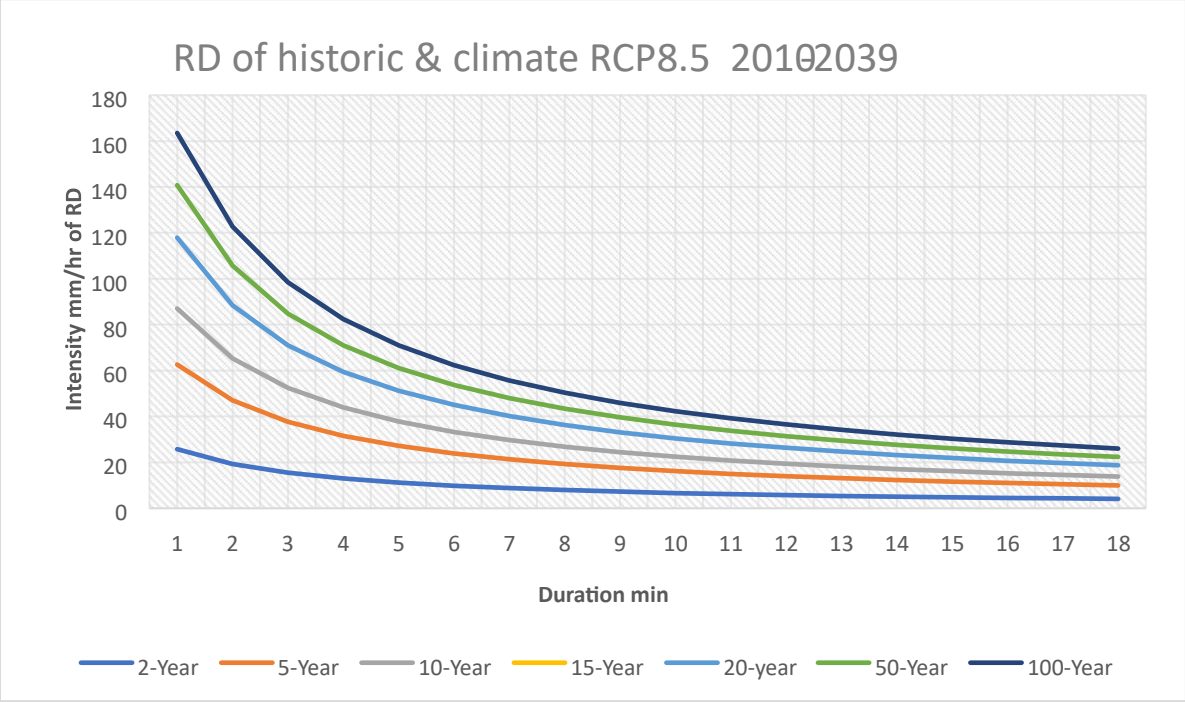

Figure 8:- Comparison between historic and climate RCP 8.5 (2010-2039)

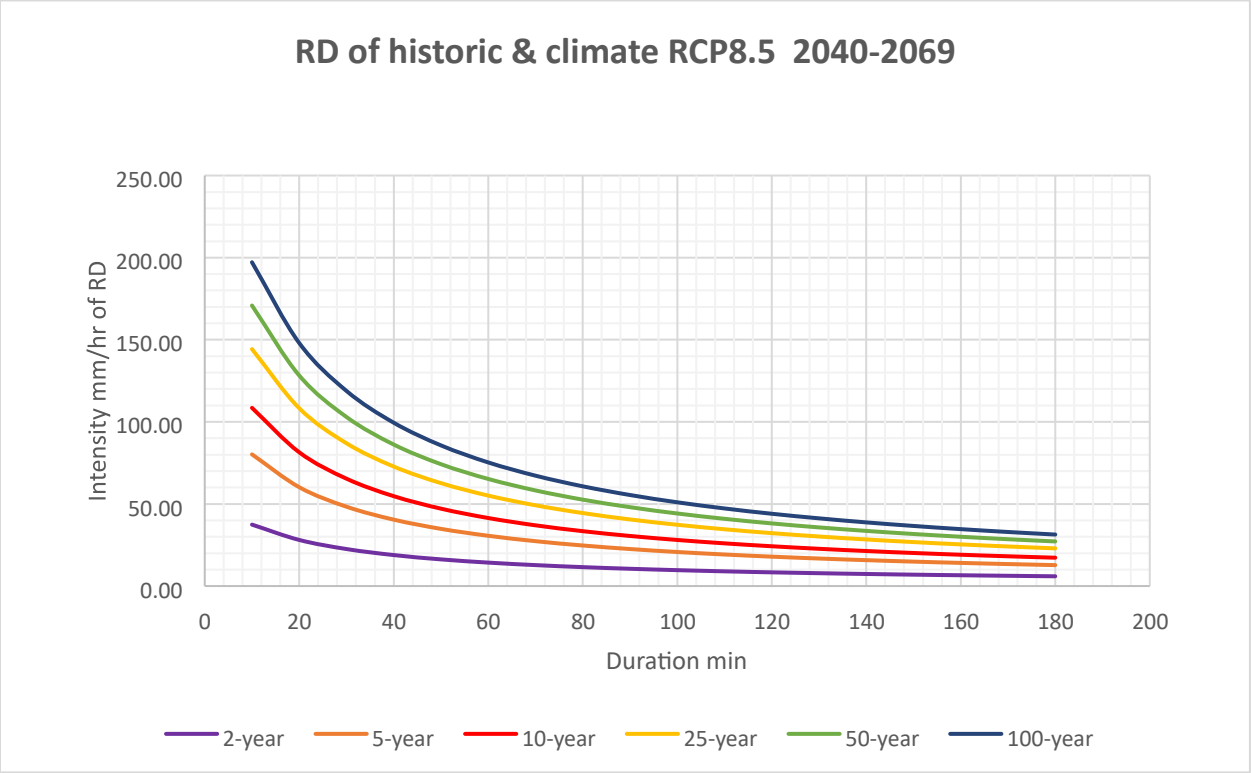

Figure 9:-Comparison between historic and climate RCP 8.5 (2040-2069)

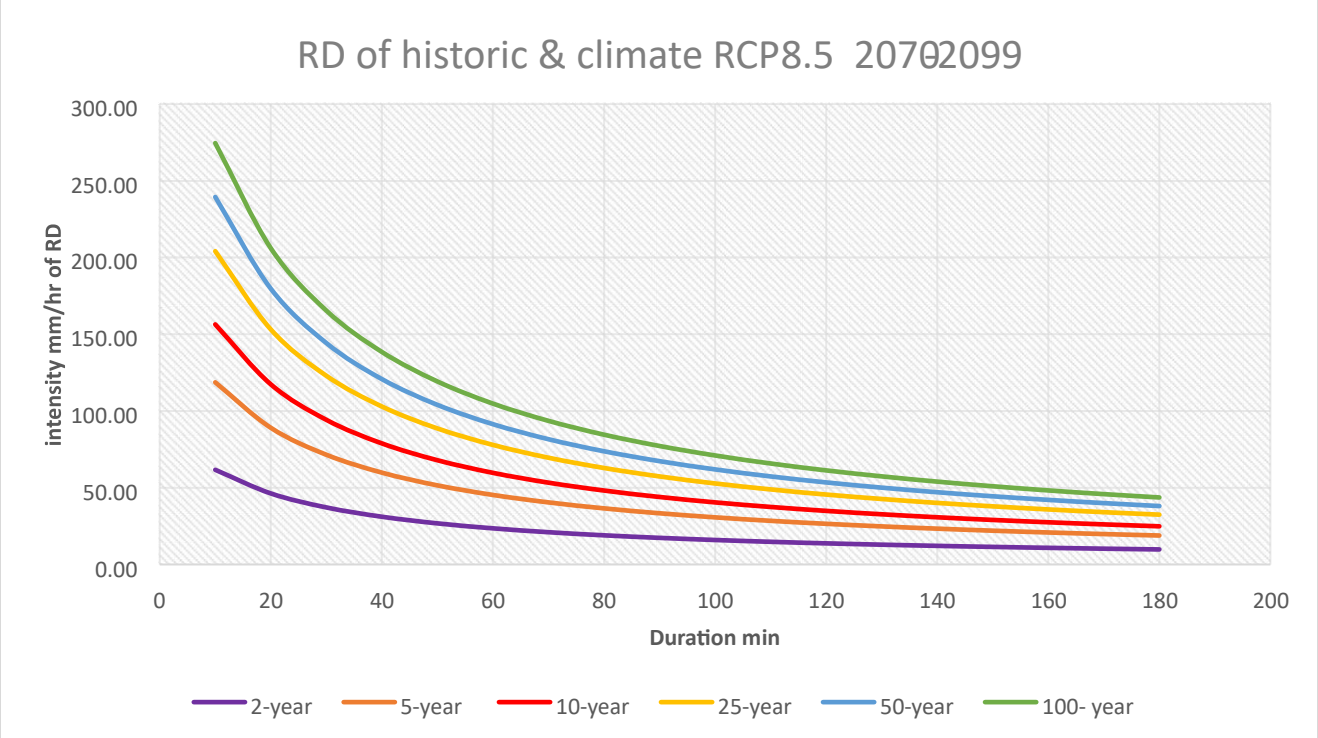

Figure 10:-Comparison between historic and climate RCP 8.5 (2070-2099) There is a significant variation between rainfall intensities during baseline and projected period of different return period. It is observed that there is significant increment of the rainfall. the figure below shows for simple demonstration, for 2-year return period for different durations were presented three stations with their probable events expected to occur with a recurrence interval of 25, 50, 100 years. For the rest of return period, it was compiled in appendix figure 5.

Figure 11:- Comparison between intensities (mm/hr) of historical data and RCP 8.5 of 2-return periods

Validating observed and the predicted rainfall data

When analyzing the observed and predicted rainfall data from the 2010–2020-year record of the data using the coefficient of determination (R square) can be used as a measure of how well a model fits the data. And it's found that R^2= 0.3706. it shows that some variations in the independent variable, it's expected to get this result because the projected climate rainfall data is with (50*50) km and the observed rainfall data is within the boundary of Addis Ababa city so the projected climate rainfall data covers beyond the boundary of Addis Ababa city. So, the model predicts well for the future climate rainfall data.

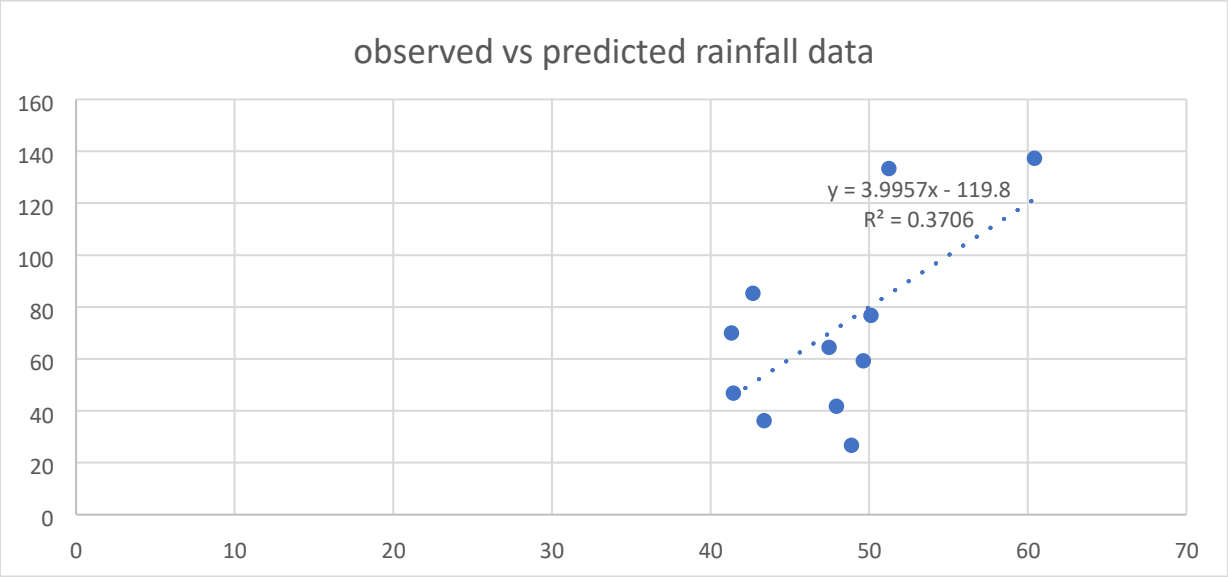

Figure 12:- R square for the observed and predicted rainfall data

5. CONCLUSIONS AND RECOMMENDATIONS

5.1. Conclusion

The atmosphere and climate are suffering significantly from the rise in greenhouse gas (GHG) emissions. Due to the effects of climate change, common weather patterns like rainfall and temperature tend to become more extreme in the future. Because of the increased risk of flooding in metropolitan areas, heavy rainfall events are becoming more common. In order to build a flood defense and water management system, IDF curves are developed. To put it another way, projects involving water are designed based on IDF curves to take safeguards and take into account potential rainfall events. It was important to update IDF curves by taking into account past and upcoming climate circumstances.

The study aimed to produce an updated IDF curve for Addis Abeba City using data from four meteorological stations in the city. The study found it difficult to obtain automatically recorded sub hourly or hourly rainfall data from the National Meteorological Agency. The general quality of the daily rainfall data for the Addis Abeba city annual maximum for a historic and climate scenario of RCP8.5 was examined, and it was discovered to be independent, stable, and homogeneous. The ideal probability distribution function was determined using EasyFit software. The generalized extreme value (GEV) distribution was found to be the best fitting function for annual maximum daily rainfall series of both historical and future climate scenario. The design rainfalls for the return periods of 2 years, 5 years, 10 years, 25 years, 50 years, and 100 years were determined using frequency analysis. The study found that future rainfall intensities increased by (27%–79% in 2010-2039; 37%–88% in 2040–2069; 55%–104% in 2069–2099), indicating that rainfall events will be more intensified in the future compared to historical events, and as a result, rainfall events will be more destructive. The findings of the study generally support the hypothesis that, extreme events like torrential rain will become more frequent in the future due to climate change.

5.2. Recommendation

Ensuring that various water management infrastructures in rural and urban watersheds surrounding the study area are carefully designed. Using IDF curves that take into account climate changes should be used to determine future design rainfalls.

Collecting Rainfall records with a shorter time span are needed for flood and other hydrological risk calculations.

Improving the collection of fine-resolution (short-duration) precipitation data at multiple gauges by installing automatic recording gauges at more stations.

Developing IDF curves for other RCP climate change scenarios.

Updating the IDF curves presented in the ERA Drainage Design Manual and using them for future designs.

REFERENCE

Adeaboye, O.B., and M.O. Alatis, (2007). Performance of Probability Distribution and Plotting Positions in Estimating the Flood of River Osun at Apoje Sub-basin, Nigeria. Agricultural Engineering International: the CIGR journal. Department of Agricultural Engineering, Federal University of Technology, Akure, Ondo State, Nigeria. Vol. IX: 1-21.

Apipattanavis, S., B. Rajagopalan, and U. Lall, (2005). Local Polynomial Technique for Flood Frequency Analysis. Journal of Hydrology. Colorado.

Baede, A.P., M.E. Ahlonsou, Y. Ding and D. Schimel, (2001). The Climate System, An Overview. *In*: Climate Change 2001: The Scientific Basis. Contribution of Working Group I to the Third Assessment Report of the Intergovernmental Panel on Climate Change [Houghton, J.T., Y. Ding, D.J. Griggs, M. Noguer, P.J. vander Linden, X. Dai, K. Maskell, and C.A. Johnson (eds.)]. Cambridge University Press, Cambridge, United Kingdom and New York, NY, USA.

Ben-Zvi, A. (2009) Rainfall Intensity-Duration-Frequency Relationships Derived from Large Partial Duration Series. *Journal of Hydrology: Regional Studies,* 367**,** 104-114.

Bhakar, S.R., A.K. Bansal, N. Chhajed and R.C. Purohit, (2006). Frequency Analysis of Consecutive Days Maximum Rainfall at Banswara, Rajasthan, India. Department of Soil and Water Engineering, Udaipur, Rajasthan, India. Vol.1, No.3.

CGD (Centre for Global Development), (2011). Map and Vulnerability Ranking. Available: http://www.cgdev.org/section/topics/climate_change/mapping_the_impacts_of_climate_change [Accessed 24 June 2013].

Chemeda Nurgi, (2014).Rainfall intensity-duration-frequency analysis under changing climate scenario in selected stations of the central highland of Ethiopia. MSc. Thesis. Haramaya University, Haramaya Ethiopia.

Chow, V. T., Maidment, D. R. & Mays, L. W. (1987) *Applied Hydrology,* New york, St. Louis San Francisco Auckland Bogota, Mc Graw-Hill International Edition: Civil Engineering Series.

Conway, D.; Mould, C.; Bewket**,(2004).** W. Over one century of rainfall and temperature observations in Addis Ababa, Ethiopia. Int. J. Climatol., 24, 77–91. [CrossRef]

Drapela, K., & Drapelova, I. (2011). Application of Mann-Kendall test and the Sen's slope estimates for trend detection in deposition data from Bílý Kříž. *Brno, 4 (2)*, 133–146

Ekubay Tesfay, (2016). Analysis of intensity-duration-frequency relationships Under future modifications of rainfall due to changing Climate for selected cities of Tigray, Ethiopia. MSc. Thesis. Arbaminch University. Arbaminch, Ethiopia.

ERA (2013) Ethiopian Road Authority: Drainage Design Manual federal democratic republic of Ethiopia. Addis Ababa, Ethiopia.

Garg, S.K., 1999. Irrigation Engineering and Hydraulics Structures. Khanna Publisher. New Delhi.

Fiddes, D., J. A. Forsgate, and A. O. Grigg, (1974). The Prediction of Storm Rainfall In East Africa. Transport and Road Research Laboratory, Department of Environment, TRRL Laboratory Report 623. Crowthorne, Berkshire.

Giugni M, A. P. (2012). Hazard scenarios for test cities using available data, Deliverable 1.2, CLUVA Project. 7th Framework Programme., www.cluva.eu: European Commission.

Grubbs F. and G. Beck (1972). "Extension of Sample Sizes and Percentage Points for Significance Tests of Outlying Observations", *Technometrics,* 14 (4), 847-854

Hassanzadeh, E., Nazemi, A. & Elshorbagy, A. J. (2014) Quantile-Based Downscaling of Precipitation using Genetic Programming: Application to IDF Curves in the City of Saskatoon. *Hydrol. Eng.*, 943-955

Hirsch, R.M., Slack J.R. (1984). Nonparametric trend test for seasonal data with serial dependence. *Water Resources Research*. 20(6), 727-732

Hüsamettin Tayşi, (2021). Disaggregation of future climate projection data to generate future rainfall intensity-duration-frequency curves to assess climate change impacts. MSc. Thesis. Istanbul Technical University, Istanbul Turkish

IPCC, (2007a): Climate Change 2007: The Physical Science Basis. Contribution of Working Group I to the Fourth Assessment Report of the Intergovernmental Panel on Climate Change [Solomon, S., D. Qin, M. Manning, Z. Chen, M. Marquis, K.B. Averyt, M. Tignor and H.L. Miller (eds.)]. Cambridge University Press, Cambridge, United Kingdom and New York, NY, USA, 996 pp.

IPCC, (2007b): Climate Change 2007: Impacts, Adaptation and Vulnerability. Contribution of Working Group II to the Fourth Assessment Report of the Intergovernmental Panel on Climate Change, M.L. Parry, O.F. Canziani, J.P. Palutikof, P.J. van der Linden and C.E. Hanson, Eds., Cambridge University Press, Cambridge, UK, 976pp.

IPCC (2012) Managing the Risks of Extreme Events and Disasters to Advance Climate Change Adaptation. A Special Report of Working Groups I and II of the Intergovernmental Panel on Climate Change [Field, C.B., V. Barros, T.F. Stocker, D. Qin, D.J. Dokken, K.L. Ebi, M.D. Mastrandrea, K.J. Mach, G.-K. Plattner, S.K. Allen, M. Tignor, and P.M. Midgley (eds.)] Cambridge University Press, Cambridge, UK, and New York, NY, USA, pp 582.

IPCC (2014) The IPCC's fifth assessment report /What's in it for Africa? (CDKN) Climate and Development Knowledge Network, licensed under a Creative Commons Attribution.

Kidist Demessie, (2016). Validating reanalysis global precipitation products (ECMWF) using intensity-duration-frequency curves in upper Blue Nile basin. MSc. Thesis. Addis Ababa University. Addis Ababa, Ethiopia.

KIPARSKY, M., MILMAN, A. & VICUN, S. (2012) Climate and Water Knowledge of Impacts to Act on Adaptation. *Annual Reviews Environmental Resources. 10.1146/annurev-environ050311-093931. environ. annualreviews.org.*

Kolbert, E., (2006). Field notes from a catastrophe: man, nature, and climate change. Bloomsbury Publishing, New York.

Koutsoyiannis D, Onof C. (2001). Rainfall disaggregation using adjusting procedures on a Poisson cluster model. J Hydrol [Internet]. 246(1–4):109–22. Available from: https://linkinghub.elsevier.com/retrieve/pii/S0022169401003638

Koutsoyiannis D, Onof C, Wheater HS. (2003). Multivariate rainfall disaggregation at a fine timescale. Water Resour Res. 39(7).

Koutsoyiannis D, Kozonis D, Manetas A. (1998). A mathematical framework for studying rainfall intensity-duration-frequency relationships. J Hydrol. 206(1–2):118–35.

Liersch,Stefan;Rust,Henning;Dobler,Andreas;Kruschke,Tim;Fischer,Madlen(2018):Biascorrected CORDEX precipitation ,min/mean/max temperature for Ethiopia, RCP 4.5 and RCP 8.5.GFZ Data Services.https://doi.org/10.5880/PIK.2018.009

McAvaney, B.J., C. Covey, S. Joussaume, V. Kattsov, A. Kitoh, W. Ogana, A.J. Pitman, A.J. Weaver, R.A. Wood and Z.-C Zhao, (2001). Model Evaluation. In Climate Change 2001: The Scientific Basis. Contribution of Working Group I to the Third Assessment Report of the Intergovernmental Panel on Climate Change [Houghton, J.T., Y. Ding, D.J. Griggs, M. Noguer, P.J. van der Linden, X. Dai, K. Maskell, and C.A. Johnson (eds.)]. Cambridge University Press, Cambridge, United Kingdom and New York, NY, USA.

Moss, R. H., Edmonds, J. A., Hibbard, K. A., Manning, M. R., Rose, S. K., Van Vuuren, D. P. & Wilbanks, T. J. (2010) The next generation of scenarios for climate change research and assessment *Nature,* 463**,** 47-56.

NAPA (2007) Climate Change National Adaptation Program of Action (NAPA) of Ethiopia; The federal democratic republic of Ethiopia, Ministry of Water Resources; National Meteorological Agency (NMA). Addis Ababa, Ethiopia

Nguyen, V. T. V., Nguyen, T. D. & Cung, A. (2007) A statistical approach to downscaling of subdaily extreme rainfall processes for climate-related impact studies in urban areas. *Water Sci. Technol. Water Supply 7***,** 183-192. [CrossRef].

Nigatu Merra, (2011). Rainfall Intensity Duration Frequency (RIDF) Relationships under the Changing climate (Case study on Upper Blue Nile River Basin, Ethiopia). MSc. Thesis. Addis Ababa University. Addis Ababa, Ethiopia.

NMSA (National Meteorological Agency of Ethiopia), (2007). Climate Change National Adaptation Programme of Action of Ethiopia.

Onoz B., Bayazit M. (2003). The power of statistical tests for trend detection. *Turkish*

Overeem, A., Buishand, A. & Holleman, I. (2008) Rainfall depth-duration-frequency curves and their uncertainties. *Journal of Hydrology: Regional Studies,* 348**,** 124-134.

Prairie J, Rajagopalan B, Lall U, Fulp T. (2007). A stochastic nonparametric technique for spacetime disaggregation of streamflow. Water Resource Res. 43(3):1–10.

Prodanovic, P. & Simonovic, S. P. (2007). Development of rainfall intensity duration frequency curves for the City of London under the changing climate. Department of Civil and Environmental Engineering, . *Report 058* London, Ontario, Canada, The University of Western Ontario.

Rao, K.H, & Hamed, A.R. (2000). Flood Frequency Analysis. CRC press LLC, Florida

Reddi, P.J., 2002. A Text Book of Hydrology. Laxmi Publications Pvt. Ltd. New Delhi. Ruttan, J.A., 2001. Guidelines on Flood Frequency Analysis. Alberta Transportation, Transport and Civil Engineering Division, Civil Project Branch, Canada. 84p

Shrestha, A., Babel, M. S., Weesakul, S. & Vojinovic, Z. (2017) Developing Intensity-DurationFrequency (IDF) Curves under Climate Change Uncertainty: The Case of Bangkok, Thailand: *water, MDPI,* 9**,** 1-22

Slobodan P. Simonovic and Angela Peck (2010). Updated Rainfall Intensity Duration Frequency curves for the City of London under the changing climate. Department of Civil and Environmental Engineering. University of Western Ontario London, Ontario, Canada.

Subramanya, K., 1994. Engineering Hydrology. TATA McGraw-Hill. New Delhi.

Suresh, R., (2005). Watershed hydrology: Principles of Hydrology. Standard Publishers Distributors. Delhi.

Tabari H., Marofi S., Aeini A., Talaee P., & Mohammadi K. (2011). Trend Analysis of Reference Evapotranspiration in the Western half of Iran. *Agricultural and Forest Meteorology, 151*, 128-136

Taylor, K., Stouffer, R. & Meehl, G. (2012) An overview of CMIP5 and the experiment design. *Bull Am Meteorol Soc,* 93(4)**,** 485-498.

USACE (2000). Hydrologic Modeling System HECHMS, Technical reference manual. Hydrologic Engineering Center, Davis

Vieux B. E. (2001). Distributed Hydrologic Modeling Using GIS. *Water Science and Technology. Kluwer*, Amsterdam

World Bank. Enhancing Urban Resilience Addis Ababa, Ethiopia. (2015). Available online: https://www.gfdrr.org/sites/default/files/publication/Addis_Ababa_Resilient_cities_program.pdf (accessed on 14 August 2017).

Woldegerima, T.; Yeshitela, K.; Lindley, S. (2016). Characterizing the urban environment through urban morphology types (UMTs) mapping and land surface cover analysis: The case of Addis Ababa, Ethiopia. Urban Ecosyst., 19, 247–259. [CrossRef]

Wozader Wolde, (2018). Development of rainfall intensity-duration-frequency (IDF) curve under changing climate: case study in omo-gibe basin, Ethiopia. MSc. Thesis. Jimma University, Jimma, Ethiopia.

APPENDIX

Appendix Tables 1:-Maximum annual rainfall for RCP 8.5 from (2010-2039)

YEAR	Max daily Annual rainfall		

2010	137.3635	2025	51.67442
2011	133.3564	2026	66.43367
2012	41.71796	2027	32.84821
2013	46.79809	2028	74.08391
2014	69.95309	2029	56.89072
2015	76.82114	2030	90.8889
2016	85.29254	2031	75.67631
2017	26.74668	2032	33.86743
2018	36.19859	2033	61.4491
2019	59.23056	2034	65.95731
2020	64.44538	2035	79.48636
2021	158.9373	2036	83.63871
2022	56.00762	2037	104.2372
2023	39.70368	2038	31.46709
2024	61.09091	2039	40.96081

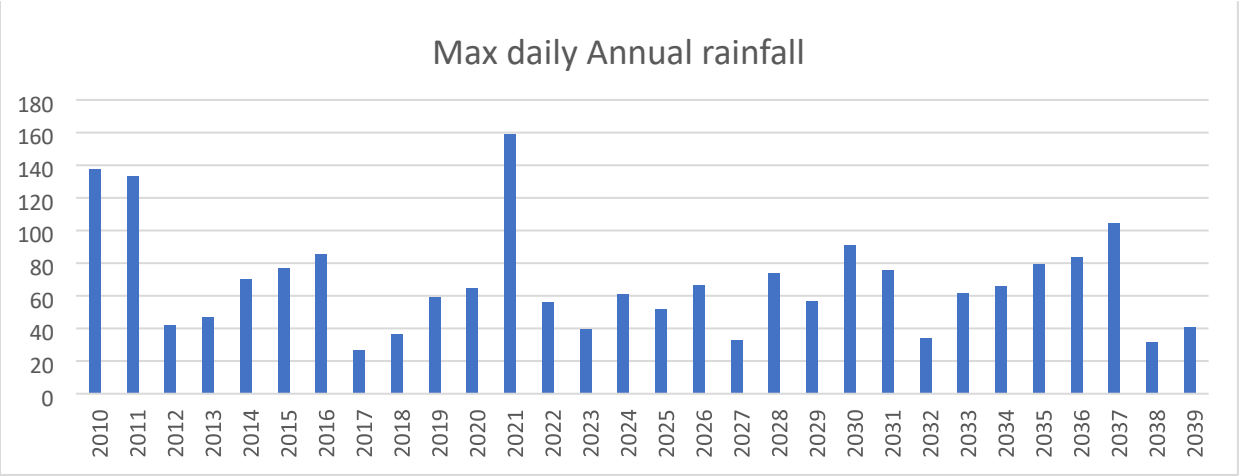

Appendix Figures 1:- maximum daily annual rainfall RCP 8.5 (2010-2039)

Appendix Tables 2:-Maximum annual rainfall for RCP 8.5 from (2040-2069)

YEAR	Max daily Annual rainfall		
2040	59.1395	2055	36.40946
2041	92.7594	2056	45.72754
2042	43.07895	2057	27.55169

2043	41.89969	2058	43.12625
2044	133.3006	2059	42.61383
2045	82.57286	2060	57.02688
2046	160.9246	2061	79.06341
2047	113.6183	2062	100.4919
2048	52.48903	2063	97.04432
2049	128.1194	2064	63.85961
2050	87.56302	2065	24.96558
2051	93.03674	2066	39.42368
2052	52.77487	2067	38.89961
2053	109.3304	2068	103.9863
2054	88.39632	2069	127.4234

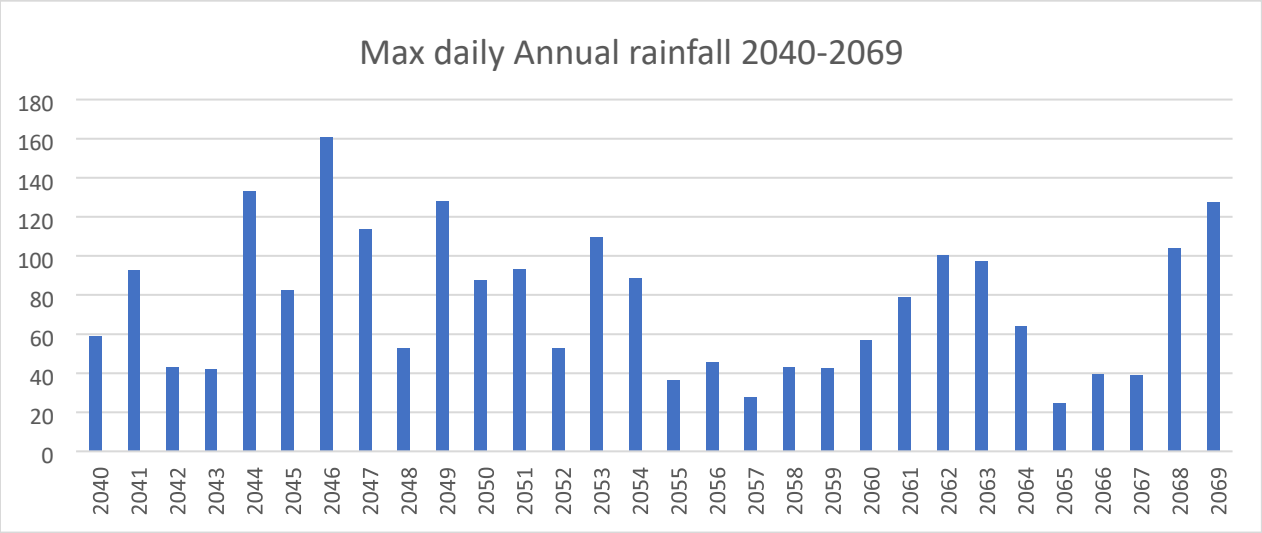

Appendix Figures 2:- maximum daily annual rainfall RCP 8.5 (2040-2069) Appendix Tables 3:- Maximum annual rainfall for RCP 8.5 from (2070-2099)

YEAR	Max daily Annual rainfall		
2070	40.24	2085	55.02
2071	48.68	2086	162.47
2072	52.16	2087	63.87
2073	116.42	2088	154.96
2074	94.69	2089	149.63
2075	38.07	2090	36.44

2076	133.28	2091	36.90
2077	129.09	2092	52.90
2078	52.63	2093	115.82
2079	177.33	2094	109.06
2080	110.50	2095	123.74
2081	75.54	2096	101.69
2082	32.33	2097	73.35
2083	64.65	2098	60.58
2084	95.28	2099	181.05

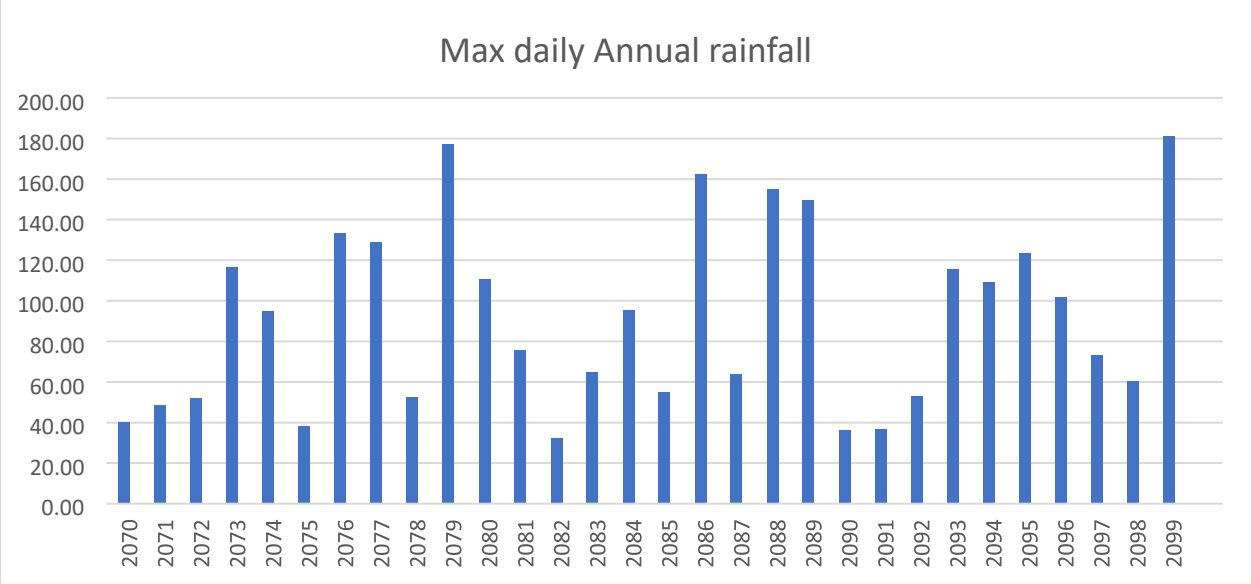

Appendix Figures 3:- maximum daily annual rainfall RCP 8.5 (2040-2069)

						Test for	
YEAR	Average Annual RF	$X_i = \ln Y_i$	X_{mean}	$X_i - X_{mean}$	$(X_i - X_{mean})_2$	High Outlier	Low Outlier
1992	45.00	3.81	3.88	-0.07	0.01	OK	OK
1993	49.55	3.90	3.88	0.02	0.00	OK	OK
1994	48.10	3.87	3.88	-0.01	0.00	OK	OK
1995	64.67	4.17	3.88	0.29	0.08	OK	OK
1996	54.07	3.99	3.88	0.11	0.01	OK	OK
1997	53.10	3.97	3.88	0.09	0.01	OK	OK
1998	62.76	4.14	3.88	0.26	0.07	OK	OK
1999	41.78	3.73	3.88	-0.15	0.02	OK	OK

2000	43.07	3.76	3.88	-0.12	0.01	OK	OK
2001	55.38	4.01	3.88	0.13	0.02	OK	OK
2002	32.54	3.48	3.88	-0.40	0.16	OK	OK
2003	46.52	3.84	3.88	-0.04	0.00	OK	OK
2004	36.68	3.60	3.88	-0.28	0.08	OK	OK
2005	47.90	3.87	3.88	-0.01	0.00	OK	OK
2006	61.93	4.13	3.88	0.25	0.06	OK	OK
2007	59.65	4.09	3.88	0.21	0.04	OK	OK
2008	44.42	3.79	3.88	-0.09	0.01	OK	OK
2009	54.95	4.01	3.88	0.13	0.02	OK	OK
2010	60.43	4.10	3.88	0.22	0.05	OK	OK
2011	51.24	3.94	3.88	0.06	0.00	OK	OK
2012	47.92	3.87	3.88	-0.01	0.00	OK	OK
2013	41.44	3.72	3.88	-0.16	0.02	OK	OK
2014	41.33	3.72	3.88	-0.16	0.03	OK	OK
2015	50.11	3.91	3.88	0.03	0.00	OK	OK
2016	42.68	3.75	3.88	-0.13	0.02	OK	OK
2017	48.88	3.89	3.88	0.01	0.00	OK	OK
2018	43.37	3.77	3.88	-0.11	0.01	OK	OK
2019	49.64	3.90	3.88	0.02	0.00	OK	OK
2020	47.48	3.86	3.88	-0.02	0.00	OK	OK
2021	44.95	3.81	3.88	-0.08	0.01	OK	OK

Appendix Tables 4:- computed outlier test for historical rainfall

Sub Data	S.no	YEAR	Max daily Annual rainfall	Rank	J	T
P	1	1992	45.00	11	1	0
	2	1993	49.55	18	1	0
	3	1994	48.10	16	1	0
	4	1995	64.67	30	1	0
	5	1996	54.07	23	1	0
	6	1997	53.10	22	1	0

	7	1998	62.76	29	1	0
	8	1999	41.78	5	1	0
	9	2000	43.07	7	1	0
	10	2001	55.38	25	1	0
	11	2002	32.54	1	1	0
	12	2003	46.52	12	1	0
	13	2004	36.68	2	1	0
	14	2005	47.90	14	1	0
	15	2006	61.93	28	1	0
q	16	2007	59.65	26	1	0
	17	2008	44.42	9	1	0
	18	2009	54.95	24	1	0
	19	2010	60.43	27	1	0
	20	2011	51.24	21	1	0
	21	2012	47.92	15	1	0
	22	2013	41.44	4	1	0
	23	2014	41.33	3	1	0
	24	2015	50.11	20	1	0
	25	2016	42.68	6	1	0
	26	2017	48.88	17	1	0
	27	2018	43.37	8	1	0
	28	2019	49.64	19	1	0
	29	2020	47.48	13	1	0
	30	2021	44.95	10	1	0
					∑T=	0

Appendix Tables 5:- computed homogeneity and stationery (M-W) test for historic rainfall

Sub Data	S.no	YEAR	Max daily Annual rainfall	Rank	J	T
p	1	2010	137.4	29	1	0
	2	2011	133.4	28	1	0
	3	2012	41.7	8	1	0
	4	2013	46.8	9	1	0
	5	2014	70.0	19	1	0
	6	2015	76.8	22	1	0
	7	2016	85.3	25	1	0
	8	2017	26.7	1	1	0
	9	2018	36.2	5	1	0
	10	2019	59.2	13	1	0
	11	2020	64.4	16	1	0
	12	2021	158.9	30	1	0
	13	2022	56.0	11	1	0
	14	2023	39.7	6	1	0
	15	2024	61.1	14	1	0
q	16	2025	51.7	10	1	0
	17	2026	66.4	18	1	0
	18	2027	32.8	3	1	0
	19	2028	74.1	20	1	0
	20	2029	56.9	12	1	0

	21	2030	90.9	26	1	0
	22	2031	75.7	21	1	0
	23	2032	33.9	4	1	0
	24	2033	61.4	15	1	0
	25	2034	66.0	17	1	0
	26	2035	79.5	23	1	0
	27	2036	83.6	24	1	0
	28	2037	104.2	27	1	0
	29	2038	31.5	2	1	0
	30	2039	41.0	7	1	0
					∑T=	0

Appendix Tables 6:- computed homogeneity and stationery (M-W) test for Climate RCP 8.5 rainfall data

YEAR	Average Annual RF	R Calculation	MEAN		
1992	45.00	2229.71	49.05	-4.05	16.44
1993	49.55	2383.31	49.05	0.50	0.25
1994	48.10	3110.47	49.05	-0.96	0.91
1995	64.67	3496.58	49.05	15.62	244.09
1996	54.07	2870.77	49.05	5.01	25.15
1997	53.10	3332.57	49.05	4.05	16.39
1998	62.76	2621.90	49.05	13.71	188.02
1999	41.78	1799.19	49.05	-7.27	52.92
2000	43.07	2384.97	49.05	-5.98	35.78
2001	55.38	1801.93	49.05	6.33	40.02
2002	32.54	1513.77	49.05	-16.51	272.59
2003	46.52	1706.22	49.05	-2.53	6.40
2004	36.68	1756.85	49.05	-12.37	153.10
2005	47.90	2966.55	49.05	-1.15	1.32
2006	61.93	3693.96	49.05	12.88	165.91
2007	59.65	2649.40	49.05	10.60	112.28
2008	44.42	2440.83	49.05	-4.63	21.45
2009	54.95	3320.50	49.05	5.90	34.82
2010	60.43	3096.00	49.05	11.38	129.43

2011	51.24	2455.46	49.05	2.19	4.78
2012	47.92	1985.80	49.05	-1.13	1.27
2013	41.44	1712.46	49.05	-7.61	57.98
2014	41.33	2070.80	49.05	-7.72	59.63
2015	50.11	2138.42	49.05	1.06	1.12
2016	42.68	2086.15	49.05	-6.37	40.61
2017	48.88	2120.17	49.05	-0.17	0.03
2018	43.37	2152.98	49.05	-5.68	32.22
2019	49.64	2356.82	49.05	0.59	0.35
2020	47.48	2134.10	49.05	-1.57	2.46
2021	44.95	2022.41	49.05	-4.10	16.84
	sum	72411.04		sum	1734.56
	Mean	49.050		variance	5784.935
				standard deviation	76.059

Appendix Tables 7:- Test for independence and stationarity for historic Appendix Tables 8:- R calculation for independence and stationarity for historic

		Average R calculation			
S	YEAR	Max daily Annual rainfall	X2	X3	X4
1	1992	45.00	2024.58	91096.88	4098937.99
2	1993	49.55	2455.61	121685.68	6030027.70
3	1994	48.10	2313.13	111250.01	5350570.16
4	1995	64.67	4182.66	270507.52	17494671.58
5	1996	54.07	2923.03	158033.89	8544113.09
6	1997	53.10	2819.45	149708.30	7949281.00
7	1998	62.76	3939.07	247223.78	15516257.99
8	1999	41.78	1745.17	72904.92	3045620.67
9	2000	43.07	1854.88	79886.63	3440583.75
10	2001	55.38	3066.54	169814.18	9403696.65

11	2002	32.54	1058.83	34454.18	1121129.68
12	2003	46.52	2164.16	100677.91	4683590.25
13	2004	36.68	1345.19	49337.08	1809524.99
14	2005	47.90	2294.50	109908.84	5264739.15
15	2006	61.93	3835.44	237532.05	14710574.19
16	2007	59.65	3557.70	212204.11	12657221.42
17	2008	44.42	1973.00	87637.40	3892715.49
18	2009	54.95	3019.60	165929.49	9117968.60
19	2010	60.43	3651.38	220640.99	13332602.13
20	2011	51.24	2625.10	134498.68	6891134.33
21	2012	47.92	2296.78	110072.76	5275210.44
22	2013	41.44	1716.92	71141.67	2947804.95
23	2014	41.33	1708.01	70588.49	2917282.75
24	2015	50.11	2510.66	125800.65	6303433.41
25	2016	42.68	1821.37	77731.71	3317398.48
26	2017	48.88	2389.41	116798.04	5709271.86
27	2018	43.37	1881.28	81598.01	3539207.80
28	2019	49.64	2463.93	122304.64	6070958.07
29	2020	47.48	2254.37	107038.11	5082194.34
30	2021	44.95	2020.24	90803.56	4081349.67
	sum	1471.50	73911.99	3798810.16	199599072.57

Appendix Tables 9:- Test for independence and stationarity for climate RCP 8.5 (2010-2039)

YEAR	Max Annual RF	R Calculation	MEAN

2010	137.36	18318.30	68.11
2011	133.36	5563.36	68.11
2012	41.72	1952.32	68.11
2013	46.80	3273.67	68.11
2014	69.95	5373.88	68.11
2015	76.82	6552.27	68.11
2016	85.29	2281.29	68.11
2017	26.75	968.19	68.11
2018	36.20	2144.06	68.11
2019	59.23	3817.14	68.11
2020	64.45	10242.78	68.11
2021	158.94	8901.70	68.11
2022	56.01	2223.71	68.11
2023	39.70	2425.53	68.11
2024	61.09	3156.84	68.11
2025	51.67	3432.92	68.11
2026	66.43	2182.23	68.11
2027	32.85	2433.52	68.11
2028	74.08	4214.69	68.11
2029	56.89	5170.73	68.11
2030	90.89	6878.14	68.11
2031	75.68	2562.96	68.11
2032	33.87	2081.12	68.11
2033	61.45	4053.02	68.11
2034	65.96	5242.71	68.11

2035	79.49	6648.14	68.11
2036	83.64	8718.26	68.11
2037	104.24	3280.04	68.11
2038	31.47	1288.92	68.11
2039	40.96	5626.52	68.11
	sum	141008.96	
	mean	68.11	

Appendix Tables 10:- R calculation for independence and stationarity for RCP 8.5(2010-2039)

		Average R calculation			
S	YEAR	Max daily Annual rainfall	X2	X3	X4
1	2010	137.36	18868.73	2591874.95	356029014.54
2	2011	133.36	17783.93	2371601.69	316268303.76
3	2012	41.72	1740.39	72605.44	3028950.56
4	2013	46.80	2190.06	102490.66	4796366.81
5	2014	69.95	4893.43	342310.89	23945704.15
6	2015	76.82	5901.49	453358.91	34827546.25
7	2016	85.29	7274.82	620487.65	52922967.91
8	2017	26.75	715.38	19134.17	511775.67
9	2018	36.20	1310.34	47432.38	1716985.14
10	2019	59.23	3508.26	207796.12	12307880.11
11	2020	64.45	4153.21	267655.05	17249131.98
12	2021	158.94	25261.07	4014925.52	638121421.67
13	2022	56.01	3136.85	175687.71	9839851.04
14	2023	39.70	1576.38	62588.18	2484980.94
15	2024	61.09	3732.10	227997.32	13928563.55
16	2025	51.67	2670.25	137983.37	7130210.16
17	2026	66.43	4413.43	293200.56	19478390.43

18	2027	32.85	1079.00	35443.37	1164251.10
19	2028	74.08	5488.42	406603.95	30122808.76
20	2029	56.89	3236.55	184129.90	10475283.17
21	2030	90.89	8260.79	750814.23	68240676.82
22	2031	75.68	5726.90	433390.95	32797428.23
23	2032	33.87	1147.00	38846.05	1315615.98
24	2033	61.45	3775.99	232031.25	14258110.12
25	2034	65.96	4350.37	286938.49	18925690.79
26	2035	79.49	6318.08	502201.26	39918149.56
27	2036	83.64	6995.43	585088.95	48936082.49
28	2037	104.24	10865.39	1132578.29	118056791.37
29	2038	31.47	990.18	31158.02	980452.19
30	2039	40.96	1677.79	68723.56	2814972.88
	sum	2043.22	169042.04	16697078.86	1902594358.12

Appendix Tables 11:- Test for independence and stationarity for RCP 8.5(2040-2069)

Test for Independence and Stationarity			
W-W Test			
YEAR	Max Annual RF	R Calculation	MEAN
2040	59.14	5485.74	75.55
2041	92.76	3995.98	75.55
2042	43.08	1804.99	75.55
2043	41.90	5585.25	75.55
2044	133.30	11007.01	75.55
2045	82.57	13288.00	75.55
2046	160.92	18283.97	75.55
2047	113.62	5963.71	75.55
2048	52.49	6724.86	75.55

2049	128.12	11218.52	75.55
2050	87.56	8146.58	75.55
2051	93.04	4910.00	75.55
2052	52.77	5769.90	75.55
2053	109.33	9664.41	75.55
2054	88.40	3218.46	75.55
2055	36.41	1664.92	75.55
2056	45.73	1259.87	75.55
2057	27.55	1188.20	75.55
2058	43.13	1837.77	75.55
2059	42.61	2430.13	75.55
2060	57.03	4508.74	75.55
2061	79.06	7945.23	75.55
2062	100.49	9752.16	75.55
2063	97.04	6197.21	75.55
2064	63.86	1594.29	75.55
2065	24.97	984.24	75.55
2066	39.42	1533.57	75.55
2067	38.90	4045.03	75.55
2068	103.99	13250.29	75.55
2069	127.42	7535.76	75.55
	sum	180794.8	
	mean	75.55	

Appendix Tables 12:- R calculation for independence and stationarity for RCP 8.5(2040-2069)

		Average R calculation			

S	YEAR	Max daily Annual rainfall	X2	X3	X4
1	2040	59.14	3497.48	206839.21	12232366.81
2	2041	92.76	8604.31	798130.20	74034076.06
3	2042	43.08	1855.80	79945.71	3443976.95
4	2043	41.90	1755.58	73558.44	3082075.75
5	2044	133.30	17769.04	2368623.24	315738820.68
6	2045	82.57	6818.28	563004.55	46488892.83
7	2046	160.92	25896.72	4167417.83	670639907.71
8	2047	113.62	12909.11	1466710.63	166645114.87
9	2048	52.49	2755.10	144612.42	7590565.52
10	2049	128.12	16414.58	2103025.32	269438303.90
11	2050	87.56	7667.28	671370.41	58787220.50
12	2051	93.04	8655.83	805310.54	74923463.26
13	2052	52.77	2785.19	146987.89	7757267.07
14	2053	109.33	11953.15	1306842.67	142877686.75
15	2054	88.40	7813.91	690720.83	61057179.95
16	2055	36.41	1325.65	48266.17	1757345.32
17	2056	45.73	2091.01	95616.64	4372313.46
18	2057	27.55	759.10	20914.36	576225.77
19	2058	43.13	1859.87	80209.38	3459129.74
20	2059	42.61	1815.94	77384.12	3297634.06
21	2060	57.03	3252.07	185455.17	10575930.50
22	2061	79.06	6251.02	494227.18	39075286.06
23	2062	100.49	10098.61	1014828.29	101981976.17
24	2063	97.04	9417.60	913924.45	88691172.32

25	2064	63.86	4078.05	260422.61	16630484.88
26	2065	24.97	623.28	15560.55	388478.14
27	2066	39.42	1554.23	61273.33	2415620.15
28	2067	38.90	1513.18	58862.08	2289711.50
29	2068	103.99	10813.16	1124420.55	116924368.06
30	2069	127.42	16236.73	2068939.41	263631334.99
	sum	2266.62	208840.83	22113404.17	2570803929.72

Appendix Tables 13:- Test for independence and stationarity for RCP 8.5(2070-2099)

Test for Independence and Stationarity			
W-W Test			
YEAR	Max Annual RF	R Calculation	MEAN
2070	40.24	1958.84	91.28
2071	48.68	2539.36	91.28
2072	52.16	6072.90	91.28
2073	116.42	11023.69	91.28
2074	94.69	3604.97	91.28
2075	38.07	5074.39	91.28
2076	133.28	17205.53	91.28
2077	129.09	6793.59	91.28
2078	52.63	9332.02	91.28
2079	177.33	19594.53	91.28
2080	110.50	8346.69	91.28
2081	75.54	2442.17	91.28
2082	32.33	2090.33	91.28
2083	64.65	6160.19	91.28
2084	95.28	5242.54	91.28
2085	55.02	8939.65	91.28
2086	162.47	10377.90	91.28
2087	63.87	9898.14	91.28
2088	154.96	23186.60	91.28
2089	149.63	5453.07	91.28
2090	36.44	1344.72	91.28
2091	36.90	1952.03	91.28

2092	52.90	6127.25	91.28
2093	115.82	12631.26	91.28
2094	109.06	13495.60	91.28
2095	123.74	12583.64	91.28
2096	101.69	7458.69	91.28
2097	73.35	4443.47	91.28
2098	60.58	10968.55	91.28
2099	181.05	7285.20	91.28
	sum	243627.49	

Appendix Tables 14:- R calculation for independence and stationarity for RCP 8.5(2070-2099)

		Average R calculation			
S	YEAR	Max daily Annual rainfall	X2	X3	X4
1	2070	40.24	1619.08	65148.30	2621425.30
2	2071	48.68	2369.89	115369.75	5616372.77
3	2072	52.16	2720.95	141932.26	7403574.87
4	2073	116.42	13554.15	1578004.93	183714940.06
5	2074	94.69	8965.65	848931.24	80382841.43
6	2075	38.07	1449.51	55186.33	2101077.19
7	2076	133.28	17764.27	2367670.24	315569450.82
8	2077	129.09	16664.35	2151209.37	277700657.15
9	2078	52.63	2769.56	145752.48	7670457.21
10	2079	177.33	31444.19	5575842.76	988736781.58
11	2080	110.50	12210.38	1349254.24	149093389.28
12	2081	75.54	5705.57	430971.93	32553571.71
13	2082	32.33	1045.33	33797.06	1092710.95
14	2083	64.65	4180.00	270249.13	17472393.33
15	2084	95.28	9078.47	865005.37	82418569.84
16	2085	55.02	3027.41	166573.56	9165189.28
17	2086	162.47	26397.94	4288989.13	696851000.22
18	2087	63.87	4079.89	260599.09	16645513.57
19	2088	154.96	24013.67	3721240.08	576656138.93

20	2089	149.63	22388.01	3349834.12	501223090.06
21	2090	36.44	1328.21	48406.12	1764142.67
22	2091	36.90	1361.43	50233.62	1853500.17
23	2092	52.90	2798.82	148068.20	7833377.54
24	2093	115.82	13413.97	1553587.84	179934490.58
25	2094	109.06	11894.22	1297191.18	141472484.93
26	2095	123.74	15312.58	1894839.67	234475043.43
27	2096	101.69	10341.04	1051590.09	106937160.66
28	2097	73.35	5379.74	394585.82	28941561.59
29	2098	60.58	3670.15	222344.47	13470026.58
30	2099	181.05	32780.39	5935005.61	1074553835.31
	SUM	2738.39	309728.80	40377414.00	5745924769.01

YEAR	Average Annual RF	Rank	S
1992	45.00	11	9
1993	49.55	18	-5
1994	48.10	16	-2
1995	64.67	30	-27
1996	54.07	23	-14
1997	53.10	22	-13
1998	62.76	29	-24
1999	41.78	5	13
2000	43.07	7	10
2001	55.38	25	-15
2002	32.54	1	18
2003	46.52	12	3
2004	36.68	2	16
2005	47.90	14	1

2006	61.93	28	-16
2007	59.65	26	-13
2008	44.42	9	4
2009	54.95	24	-11
2010	60.43	27	-12
2011	51.24	21	-11
2012	47.92	15	-4
2013	41.44	4	5
2014	41.33	3	6
2015	50.11	20	-7
2016	42.68	6	4
2017	48.88	17	-3
2018	43.37	8	2
2019	49.64	19	-3
2020	47.48	13	-2
2021	44.95	10	0

Appendix Tables 15:- computed Trend test for historic

YEAR	Max daily Annual rainfall	Rank	S
2010	137.36	29	-27
2011	133.36	28	-26
2012	41.72	8	13
2013	46.80	9	12
2014	69.95	19	-7

2015	76.82	22	-12
2016	85.29	25	-17
2017	26.75	1	22
2018	36.20	5	15
2019	59.23	13	4
2020	64.45	16	-1
2021	158.94	30	-18
2022	56.01	11	5
2023	39.70	6	10
2024	61.09	14	3
2025	51.67	10	6
2026	66.43	18	-1
2027	32.85	3	10
2028	74.08	20	-1
2029	56.89	12	4
2030	90.89	26	-7
2031	75.68	21	-2
2032	33.87	4	5
2033	61.45	15	2
2034	65.96	17	1
2035	79.49	23	0
2036	83.64	24	-1
2037	104.24	27	-2
2038	31.47	2	1
2039	40.96	7	0

Appendix Tables 16:- computed trend test for climate RCP 8.5 (2010-2039)

YEAR	Max daily Annual rainfall	Rank	S
2040	59.14	14	3
2041	92.76	20	-8

2042	43.08	8	13
2043	41.90	6	16
2044	133.30	29	-23
2045	82.57	17	-2
2046	160.92	30	-23
2047	113.62	26	-18
2048	52.49	11	5
2049	128.12	28	-20
2050	87.56	18	-5
2051	93.04	21	-8
2052	52.77	12	1
2053	109.33	25	-14
2054	88.40	19	-7
2055	36.41	3	10
2056	45.73	10	1
2057	27.55	2	10
2058	43.13	9	3
2059	42.61	7	4
2060	57.03	13	3
2061	79.06	16	0
2062	100.49	23	-3
2063	97.04	22	-2
2064	63.86	15	-1
2065	24.97	1	4
2066	39.42	5	1
2067	38.90	4	2
2068	103.99	24	1
2069	127.42	27	0

Appendix Tables 17:- Test result for trend RCP 8.5 (2040-2069) Appendix Tables 18:- Test result for trend RCP 8.5 (2070-2099)

YEAR	Max daily Annual rainfall	Rank	S
2070	40.24	5	21
2071	48.68	6	20
2072	52.16	7	19
2073	116.42	22	-10
2074	94.69	16	1
2075	38.07	4	18
2076	133.28	25	-13
2077	129.09	24	-12
2078	52.63	8	15
2079	177.33	29	-18
2080	110.50	20	-7
2081	75.54	15	0
2082	32.33	1	17
2083	64.65	13	4
2084	95.28	17	1
2085	55.02	10	8
2086	162.47	28	-11
2087	63.87	12	4
2088	154.96	27	-9
2089	149.63	26	-8
2090	36.44	2	9
2091	36.90	3	8

2092	52.90	9	7
2093	115.82	21	-2
2094	109.06	19	-1
2095	123.74	23	-2
2096	101.69	18	-1
2097	73.35	14	0
2098	60.58	11	1
2099	181.05	30	0

Appendix Tables 19:- Short duration for RCP 8.5 (2039-2069)

	10	20	30	40	50	60	70	80	90	100	110	120	130	140	150	160	170	180
Year							Time in Hour											
	0.166667	0.333333	0.5	0.666667	0.833333	1	1.166667	1.333333	1.5	1.666667	1.833333	2	2.166667	2.333333	2.5	2.666667	2.833333	3
2040	101.2208	75.96296	60.98622	51.0477	43.95822	38.63932	34.49727	31.17783	28.45641	26.1836	24.25611	22.60019	21.16179	19.90035	18.78485	17.79113	16.90013	16.09656
2041	158.7633	119.1467	95.65595	80.06753	68.94779	60.60519	54.10844	48.90196	44.63345	41.06858	38.04533	35.44805	33.19195	31.2134	29.46375	27.90512	26.5076	25.24721
2042	73.73223	55.33365	44.42415	37.18464	32.02046	28.14602	25.12882	22.71085	20.72848	19.0729	17.66886	16.46264	15.41487	14.496	13.68344	12.95958	12.31055	11.72521
2043	71.71386	53.81893	43.20807	36.16674	31.14392	27.37554	24.44094	22.08916	20.16106	18.5508	17.18519	16.01199	14.9929	14.09918	13.30886	12.60483	11.97356	11.40424
2044	228.152	171.2207	137.4631	115.0616	99.08193	87.09313	77.75693	70.27491	64.14082	59.0179	54.67332	50.94088	47.69873	44.85544	42.3411	40.10126	38.09294	36.28169
2045	141.3284	106.0624	85.15132	71.27477	61.37617	53.94972	48.16643	43.5317	39.73194	36.55856	33.86731	31.55526	29.54691	27.78564	26.22813	24.84067	23.59662	22.47465
2046	275.4321	206.7029	165.9497	138.906	119.6148	105.1415	93.87057	84.83805	77.43278	71.24823	66.00332	61.49741	57.58338	54.15088	51.11548	48.41148	45.98697	43.80038
2047	194.4645	145.9393	117.1662	98.07237	84.45213	74.23352	66.27584	59.89857	54.6702	50.3037	46.60061	43.41928	40.65584	38.23238	36.08928	34.18017	32.46838	30.92457
2048	89.83815	67.42063	54.12808	45.30718	39.01494	34.29418	30.61792	27.67176	25.25638	23.23915	21.52841	20.05871	18.78207	17.66248	16.67242	15.79045	14.99965	14.28644
2049	219.2841	164.5656	132.1201	110.5894	95.23077	83.70796	74.73464	67.54344	61.64776	56.72396	52.54825	48.96089	45.84475	43.11198	40.69536	38.54259	36.61232	34.87148
2050	149.8694	112.4721	90.29731	75.58215	65.08534	57.21009	51.07729	46.16247	42.13308	38.76792	35.91403	33.46226	31.33254	29.46483	27.81319	26.34188	25.02264	23.83287
2051	159.238	119.503	95.94195	80.30692	69.15394	60.78639	54.27022	49.04817	44.76689	41.19137	38.15908	35.55404	33.29119	31.30672	29.55184	27.98856	26.58685	25.3227
2052	90.32739	67.78778	54.42285	45.55391	39.22741	34.48094	30.78466	27.82246	25.39392	23.36571	21.64565	20.16795	18.88435	17.75867	16.76321	15.87644	15.08133	14.36424
2053	187.1257	140.4318	112.7444	94.37123	81.265	71.43203	63.77467	57.63807	52.60701	48.40529	44.84196	41.78069	39.12154	36.78953	34.72732	32.89025	31.24306	29.75751
2054	151.2957	113.5425	91.15663	76.30143	65.70473	57.75453	51.56337	46.60178	42.53404	39.13686	36.25581	33.7807	31.63071	29.74523	28.07788	26.59256	25.26077	24.05967
2055	62.317	46.76689	37.5464	31.42771	27.06305	23.78845	21.23838	19.19476	17.5193	16.12004	14.93337	13.9139	13.02834	12.25173	11.56497	10.95318	10.40463	9.909913
2056	78.26545	58.73569	47.15545	39.47084	33.98915	29.8765	26.6738	24.10717	22.00292	20.24555	18.75518	17.4748	16.36261	15.38725	14.52473	13.75637	13.06743	12.4461

2057	47.15638	35.38934	28.41203	23.78191	20.47909	18.00114	16.07146	14.52501	13.25717	12.19832	11.30034	10.52889	9.858776	9.271102	8.751415	8.288467	7.873369	7.499006
2058	73.81319	55.39441	44.47293	37.22547	32.05562	28.17693	25.15642	22.73579	20.75125	19.09385	17.68826	16.48072	15.4318	14.51192	13.69846	12.97382	12.32407	11.73809
2059	72.93616	54.73623	43.94452	36.78317	31.67474	27.84213	24.85752	22.46565	20.50469	18.86698	17.47809	16.2849	15.24844	14.33949	13.5357	12.81966	12.17764	11.59862
2060	97.60497	73.24937	58.80764	49.22414	42.38792	37.25903	33.26494	30.06408	27.43988	25.24826	23.38962	21.79286	20.40584	19.18946	18.11381	17.15559	16.29642	15.52155
2061	135.3218	101.5546	81.53228	68.24551	58.76761	51.65679	46.1193	41.68155	38.04329	35.00477	32.42791	30.21413	28.29113	26.60472	25.11341	23.78491	22.59373	21.51945
2062	171.9979	129.0789	103.6299	86.74199	74.69531	65.65726	58.61894	52.97844	48.35411	44.49207	41.2168	38.40302	35.95884	33.81536	31.91986	30.2313	28.71728	27.35183
2063	166.0972	124.6506	100.0747	83.76616	72.13276	63.40478	56.60792	51.16093	46.69524	42.9657	39.80279	37.08554	34.72521	32.65527	30.8248	29.19417	27.73209	26.41348
2064	109.2996	82.02582	65.85372	55.12197	47.46666	41.72325	37.25061	33.66623	30.72761	28.2734	26.19206	24.40398	22.85078	21.48866	20.28413	19.2111	18.24898	17.38128
2065	42.73016	32.06756	25.74517	21.54965	18.55684	16.31149	14.56293	13.16164	12.0128	11.05334	10.23965	9.54061	8.933393	8.400881	7.929974	7.51048	7.134345	6.795121
2066	67.47602	50.63857	40.65474	34.02951	29.30351	25.75782	22.99663	20.78383	18.96967	17.45456	16.16965	15.06578	14.10691	13.26601	12.52239	11.85996	11.266	10.73032
2067	66.57903	49.96541	40.1143	33.57714	28.91396	25.41541	22.69093	20.50754	18.71749	17.22253	15.9547	14.86551	13.91938	13.08966	12.35593	11.7023	11.11623	10.58768
2068	177.9789	133.5674	107.2335	89.75833	77.29274	67.94041	60.65734	54.8207	50.03556	46.03922	42.65007	39.73843	37.20926	34.99125	33.02983	31.28256	29.71589	28.30296
2069	218.0929	163.6717	131.4024	109.9886	94.71346	83.25324	74.32867	67.17653	61.31289	56.41583	52.26281	48.69493	45.59572	42.87779	40.4743	38.33322	36.41344	34.68205
	10	20	30	40	50	60	70	80	90	100	110	120	130	140	150	160	170	180
Year							Time in Hour											
	0.166667	0.333333	0.5	0.666667	0.833333	1	1.166667	1.333333	1.5	1.666667	1.833333	2	2.166667	2.333333	2.5	2.666667	2.833333	3
avg	129.3151	97.04678	77.91319	65.21619	56.159	49.36382	44.07213	39.83137	36.3546	33.45096	30.98849	28.87296	27.03533	25.42378	23.99866	22.72914	21.59083	20.56423
std	61.62033	46.24407	37.12666	31.07637	26.7605	23.52251	21.00095	18.98017	17.32345	15.93982	14.76642	13.75835	12.88269	12.11476	11.43568	10.83073	10.28831	9.799126

Appendix Tables 20:- Short duration for RCP 8.5 (2070-2099)

	10	20	30	40	50	60	70	80	90	100	110	120	130	140	150	160	170	180
Year							Time in Hour											
	0.166667	0.333333	0.5	0.666667	0.833333	1	1.166667	1.333333	1.5	1.666667	1.833333	2	2.166667	2.333333	2.5	2.666667	2.833333	3
2070	68.87	51.68	41.49	34.73	29.91	26.29	23.47	21.21	19.36	17.82	16.50	15.38	14.40	13.54	12.78	12.10	11.50	10.95
2071	83.32	62.53	50.20	42.02	36.18	31.81	28.40	25.66	23.42	21.55	19.97	18.60	17.42	16.38	15.46	14.65	13.91	13.25
2072	89.28	67.00	53.79	45.03	38.77	34.08	30.43	27.50	25.10	23.09	21.39	19.93	18.67	17.55	16.57	15.69	14.91	14.20
2073	199.26	149.54	120.06	100.49	86.54	76.07	67.91	61.38	56.02	51.55	47.75	44.49	41.66	39.18	36.98	35.02	33.27	31.69
2074	162.06	121.62	97.64	81.73	70.38	61.86	55.23	49.92	45.56	41.92	38.84	36.18	33.88	31.86	30.08	28.49	27.06	25.77
2075	65.16	48.90	39.26	32.86	28.30	24.87	22.21	20.07	18.32	16.86	15.62	14.55	13.62	12.81	12.09	11.45	10.88	10.36
2076	228.12	171.20	137.44	115.05	99.07	87.08	77.75	70.27	64.13	59.01	54.67	50.93	47.69	44.85	42.34	40.10	38.09	36.28
2077	220.95	165.81	133.12	111.43	95.95	84.34	75.30	68.06	62.12	57.15	52.95	49.33	46.19	43.44	41.00	38.83	36.89	35.14
2078	90.07	67.60	54.27	45.43	39.12	34.38	30.70	27.74	25.32	23.30	21.58	20.11	18.83	17.71	16.72	15.83	15.04	14.32
2079	303.50	227.77	182.86	153.06	131.81	115.86	103.44	93.48	85.32	78.51	72.73	67.76	63.45	59.67	56.32	53.35	50.67	48.26
2080	189.13	141.93	113.95	95.38	82.13	72.20	64.46	58.25	53.17	48.92	45.32	42.23	39.54	37.18	35.10	33.24	31.58	30.08
2081	129.28	97.02	77.89	65.20	56.15	49.35	44.06	39.82	36.35	33.44	30.98	28.87	27.03	25.42	23.99	22.72	21.59	20.56
2082	55.34	41.53	33.34	27.91	24.03	21.12	18.86	17.04	15.56	14.31	13.26	12.36	11.57	10.88	10.27	9.73	9.24	8.80
2083	110.66	83.04	66.67	55.81	48.06	42.24	37.71	34.08	31.11	28.62	26.52	24.71	23.13	21.76	20.54	19.45	18.48	17.60
2084	163.08	122.39	98.26	82.24	70.82	62.25	55.58	50.23	45.85	42.18	39.08	36.41	34.09	32.06	30.26	28.66	27.23	25.93
2085	94.17	70.67	56.74	47.49	40.90	35.95	32.10	29.01	26.48	24.36	22.57	21.03	19.69	18.51	17.48	16.55	15.72	14.98

2086	278.08	208.69	167.55	140.24	120.77	106.15	94.77	85.66	78.18	71.93	66.64	62.09	58.14	54.67	51.61	48.88	46.43	44.22
2087	109.32	82.04	65.87	55.13	47.48	41.73	37.26	33.67	30.73	28.28	26.20	24.41	22.86	21.49	20.29	19.22	18.25	17.39
2088	265.23	199.05	159.80	133.76	115.18	101.25	90.39	81.70	74.56	68.61	63.56	59.22	55.45	52.14	49.22	46.62	44.28	42.18
2089	256.09	192.19	154.30	129.15	111.22	97.76	87.28	78.88	72.00	66.25	61.37	57.18	53.54	50.35	47.53	45.01	42.76	40.73
2090	62.38	46.81	37.58	31.46	27.09	23.81	21.26	19.21	17.54	16.14	14.95	13.93	13.04	12.26	11.58	10.96	10.41	9.92
2091	63.15	47.39	38.05	31.85	27.43	24.11	21.52	19.45	17.75	16.34	15.13	14.10	13.20	12.42	11.72	11.10	10.54	10.04
2092	90.55	67.95	54.56	45.67	39.32	34.57	30.86	27.89	25.46	23.42	21.70	20.22	18.93	17.80	16.80	15.92	15.12	14.40
2093	198.23	148.77	119.44	99.97	86.09	75.67	67.56	61.06	55.73	51.28	47.50	44.26	41.44	38.97	36.79	34.84	33.10	31.52
2094	186.66	140.09	112.47	94.14	81.06	71.26	63.62	57.50	52.48	48.29	44.73	41.68	39.02	36.70	34.64	32.81	31.17	29.68
2095	211.80	158.95	127.61	106.81	91.98	80.85	72.18	65.24	59.54	54.79	50.75	47.29	44.28	41.64	39.31	37.23	35.36	33.68
2096	174.05	130.62	104.87	87.78	75.59	66.44	59.32	53.61	48.93	45.02	41.71	38.86	36.39	34.22	32.30	30.59	29.06	27.68
2097	125.54	94.21	75.64	63.31	54.52	47.92	42.78	38.67	35.29	32.47	30.08	28.03	26.25	24.68	23.30	22.07	20.96	19.96
2098	103.69	77.82	62.47	52.29	45.03	39.58	35.34	31.94	29.15	26.82	24.85	23.15	21.68	20.39	19.24	18.23	17.31	16.49
2099	309.88	232.56	186.71	156.28	134.58	118.29	105.61	95.45	87.12	80.16	74.26	69.19	64.79	60.92	57.51	54.47	51.74	49.28

Appendix Tables 21:- Computed rainfall intensity values for historic rainfall

			Return Period			
Duration	2	5	10	25	50	100
10	81.78	93.48	101.23	111.02	118.28	125.49
20	61.37	70.15	75.97	83.32	88.77	94.18
30	49.27	56.32	60.99	66.89	71.27	75.61
40	41.24	47.14	51.05	55.99	59.65	63.29
50	35.51	40.60	43.96	48.21	51.37	54.50
60	31.22	35.68	38.64	42.38	45.15	47.90
70	27.87	31.86	34.50	37.84	40.31	42.77
80	25.19	28.79	31.18	34.20	36.43	38.65
90	22.99	26.28	28.46	31.21	33.25	35.28
100	21.15	24.18	26.19	28.72	30.60	32.46
110	19.60	22.40	24.26	26.60	28.34	30.07
120	18.26	20.87	22.60	24.79	26.41	28.02
130	17.10	19.54	21.16	23.21	24.73	26.24
140	16.08	18.38	19.90	21.83	23.25	24.67
150	15.18	17.35	18.79	20.60	21.95	23.29
160	14.37	16.43	17.79	19.51	20.79	22.06
170	13.65	15.61	16.90	18.54	19.75	20.95
180	13.00	14.87	16.10	17.65	18.81	19.96

Appendix Tables 22:- Computed rainfall intensity values for climate RCP8.5 (2010-2039)

Duration			Return Period			
	2	5	10	25	50	100
10	107.5	156.1	188.3	228.9	259.1	289.0

20	80.7	117.2	141.3	171.8	194.4	216.9
30	64.8	94.1	113.4	137.9	156.1	174.1
40	54.2	78.7	95.0	115.4	130.7	145.7
50	46.7	67.8	81.8	99.4	112.5	125.5
60	41.1	59.6	71.9	87.4	98.9	110.3
70	36.7	53.2	64.2	78.0	88.3	98.5
80	33.1	48.1	58.0	70.5	79.8	89.0
90	30.2	43.9	52.9	64.4	72.8	81.2
100	27.8	40.4	48.7	59.2	67.0	74.8
110	25.8	37.4	45.1	54.9	62.1	69.3
120	24.0	34.9	42.0	51.1	57.8	64.5
130	22.5	32.6	39.4	47.9	54.2	60.4
140	21.1	30.7	37.0	45.0	50.9	56.8
150	20.0	29.0	34.9	42.5	48.1	53.6
160	18.9	27.4	33.1	40.2	45.5	50.8
170	18.0	26.1	31.4	38.2	43.3	48.3
180	17.1	24.8	29.9	36.4	41.2	46.0

Appendix Tables 23:- Computed rainfall intensity values for RCP 8.5 (2040-2069)

Duration			Return Period			
	2	5	10	25	50	100
10	119.1874	173.6708	209.7435	255.3214	289.1338	322.6964
20	89.44632	130.3343	157.4057	191.6105	216.9855	242.1732
30	71.81122	104.6378	126.3718	153.8328	174.205	194.4267
40	60.10862	87.58565	105.7778	128.7637	145.816	162.7423
50	51.76077	75.4218	91.08747	110.8811	125.5651	140.1407
60	45.49777	66.29585	80.06599	97.4646	110.3719	123.1839
70	40.62051	59.18908	71.48309	87.0166	98.54025	109.9788
80	36.71187	53.49372	64.60476	78.64359	89.05839	99.39629
90	33.5074	48.8244	58.96559	71.77901	81.28474	90.72028
100	30.83117	44.92481	54.25602	66.04603	74.79254	83.47446
110	28.56155	41.61768	50.26199	61.18408	69.28672	77.32952
120	26.61171	38.77653	46.8307	57.00717	64.55665	72.05039
130	24.91799	36.30858	43.85014	53.37892	60.44792	67.46472
140	23.43265	34.14425	41.23627	50.19705	56.84466	63.44319

150	22.11915	32.23032	38.92479	47.38328	53.65827	59.88692
160	20.94905	30.52534	36.86568	44.87671	50.81975	56.71891
170	19.89989	28.99659	35.01939	42.62923	48.27463	53.87836
180	18.95369	27.61786	33.35429	40.60229	45.97927	51.31655

Appendix Tables 24:- Computed rainfall intensity values for RCP 8.5 (2070-2099)

Duration			Return Period			
	2	5	10	25	50	100
10	143.46	212.16	257.65	315.12	357.76	400.08
20	107.66	159.22	193.36	236.49	268.49	300.25
30	86.44	127.83	155.24	189.86	215.55	241.05
40	72.35	107.00	129.94	158.92	180.42	201.77
50	62.30	92.14	111.89	136.85	155.37	173.75
60	54.76	80.99	98.35	120.29	136.57	152.72
70	48.89	72.31	87.81	107.40	121.93	136.35
80	44.19	65.35	79.36	97.06	110.20	123.23
90	40.33	59.65	72.43	88.59	100.58	112.48
100	37.11	54.88	66.65	81.52	92.54	103.49
110	34.38	50.84	61.74	75.51	85.73	95.87
120	32.03	47.37	57.53	70.36	79.88	89.33
130	29.99	44.36	53.87	65.88	74.80	83.64
140	28.20	41.71	50.65	61.95	70.34	78.66
150	26.62	39.37	47.82	58.48	66.39	74.25
160	25.22	37.29	45.29	55.39	62.88	70.32
170	23.95	35.42	43.02	52.61	59.73	66.80
180	22.81	33.74	40.97	50.11	56.89	63.62

Relative difference (%) between IDF historical data and IDF (2040-2069) YE ،R						
Duration	2	5	10	20	50	100
10	37.41	80.19	108.51	144.30	170.85	197.20
20	28.08	60.18	81.44	108.29	128.22	147.99
30	22.54	48.32	65.38	86.94	102.94	118.82

40	18.87	40.44	54.73	72.77	86.16	99.45
50	16.25	34.83	47.13	62.67	74.20	85.64
60	14.28	30.61	41.42	55.08	65.22	75.28
70	12.75	27.33	36.98	49.18	58.23	67.21
80	11.52	24.70	33.42	44.45	52.62	60.74
90	10.52	22.54	30.51	40.57	48.03	55.44
100	9.68	20.74	28.07	37.33	44.20	51.01
110	8.96	19.22	26.00	34.58	40.94	47.26
120	8.35	17.90	24.23	32.22	38.15	44.03
130	7.82	16.77	22.69	30.17	35.72	41.23
140	7.36	15.77	21.33	28.37	33.59	38.77
150	6.94	14.88	20.14	26.78	31.71	36.60
160	6.58	14.09	19.07	25.36	30.03	34.66
170	6.25	13.39	18.12	24.09	28.53	32.93
180	5.95	12.75	17.26	22.95	27.17	31.36

Appendix Tables 25:- Relative difference between historic and RCP 8.5 (2040-2069)

Relative difference (%) between IDF historical data and IDF (2070-2099) YE ،R						
Duration	2	5	10	25	50	100
10	61.68	118.68	156.42	204.10	239.47	274.59
20	46.29	89.07	117.39	153.17	179.72	206.07
30	37.16	71.51	94.24	122.97	144.29	165.44
40	31.11	59.85	78.89	102.93	120.77	138.48
50	26.79	51.54	67.93	88.64	104.00	119.25
60	23.55	45.30	59.71	77.91	91.42	104.82

70	21.02	40.45	53.31	69.56	81.62	93.58
80	19.00	36.56	48.18	62.87	73.76	84.58
90	17.34	33.37	43.97	57.38	67.32	77.20
100	15.96	30.70	40.46	52.80	61.95	71.03
110	14.78	28.44	37.48	48.91	57.39	65.80
120	13.77	26.50	34.92	45.57	53.47	61.31
130	12.90	24.81	32.70	42.67	50.07	57.41
140	12.13	23.33	30.75	40.13	47.08	53.98
150	11.45	22.03	29.03	37.88	44.44	50.96
160	10.84	20.86	27.49	35.87	42.09	48.26
170	10.30	19.82	26.12	34.08	39.98	45.85
180	9.81	18.87	24.87	32.46	38.08	43.67

Appendix Tables 26:- Relative difference between historic and RCP 8.5 (2070-2099) Appendix Figures 4:-Comparison between intensities of historical data and climate scenario RCP 8.5 for various return period.

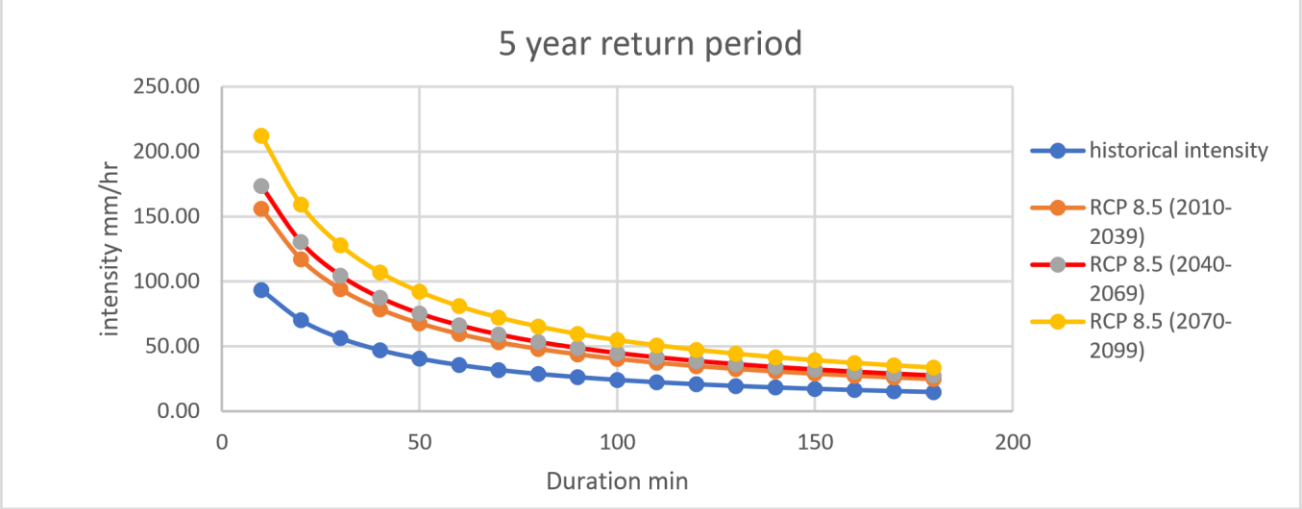
5 year return period
250.00
200.00
150.00
100.00
50.00
0.00
intensity mm/hr
0
50
100
150
200
Duration min
historical intensity
RCP 8.5 (2010-2039)
RCP 8.5 (2040-2069)
RCP 8.5 (2070-2099)

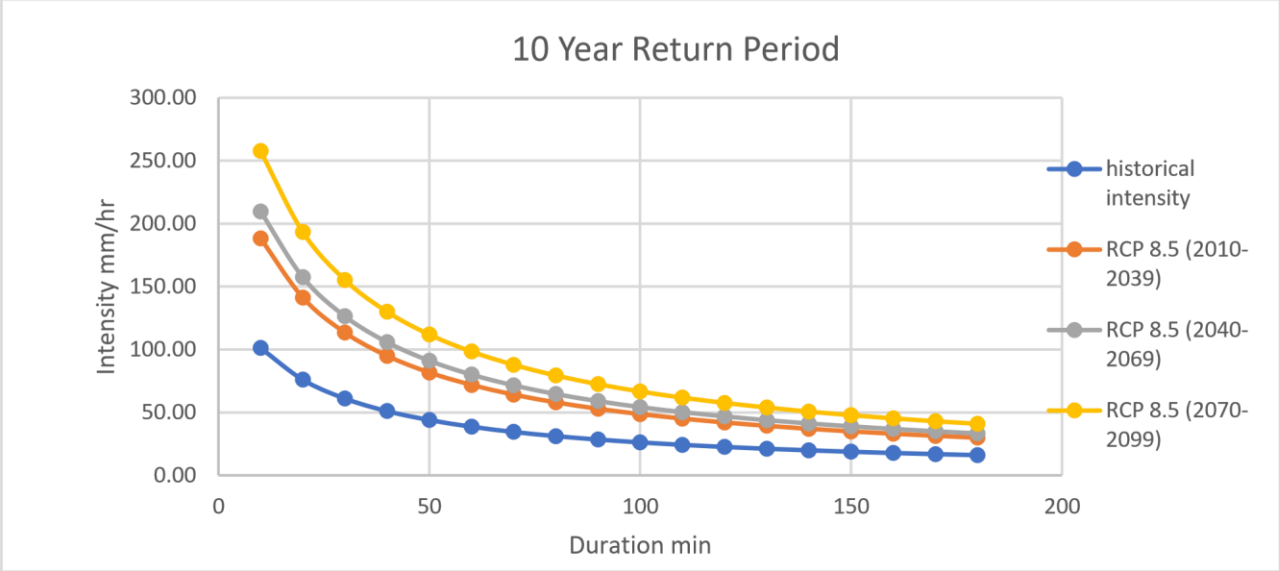
10 Year Return Period
300.00
250.00
200.00
150.00
100.00
50.00
0.00
Intensity mm/hr
0
50
100
150
200
Duration min
historical intensity
RCP 8.5 (2010-2039)
RCP 8.5 (2040-2069)
RCP 8.5 (2070-2099)

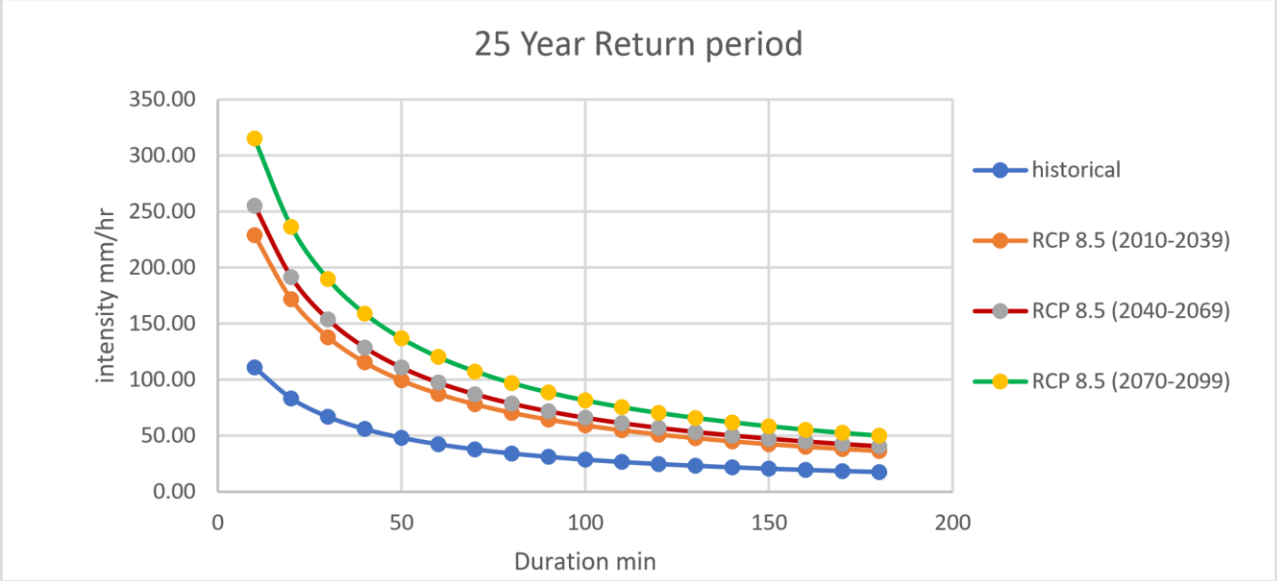
25 Year Return period
intensity mm/hr
350.00
300.00
250.00
200.00
150.00
100.00
50.00
0.00
0
50
100
150
200
Duration min
historical
RCP 8.5 (2010-2039)
RCP 8.5 (2040-2069)
RCP 8.5 (2070-2099)

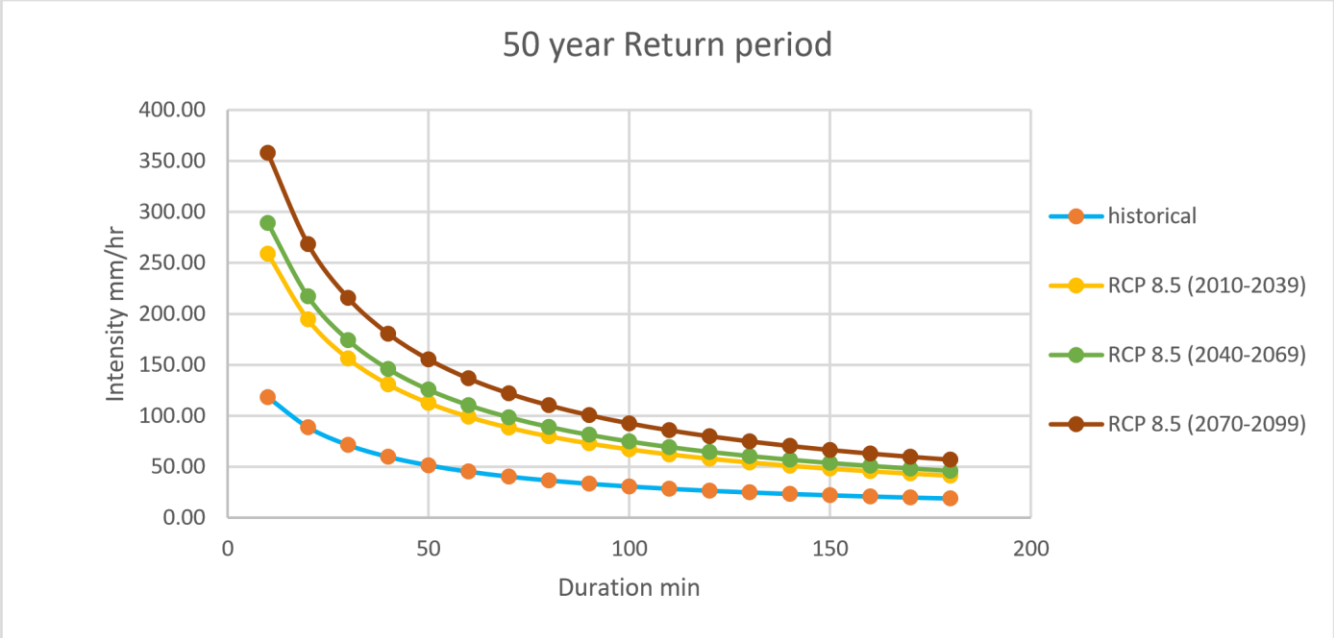
50 year Return period
Intensity mm/hr
400.00
350.00
300.00
250.00
200.00
150.00
100.00
50.00
0.00
0
50
100
150
200
Duration min
historical
RCP 8.5 (2010-2039)
RCP 8.5 (2040-2069)
RCP 8.5 (2070-2099)

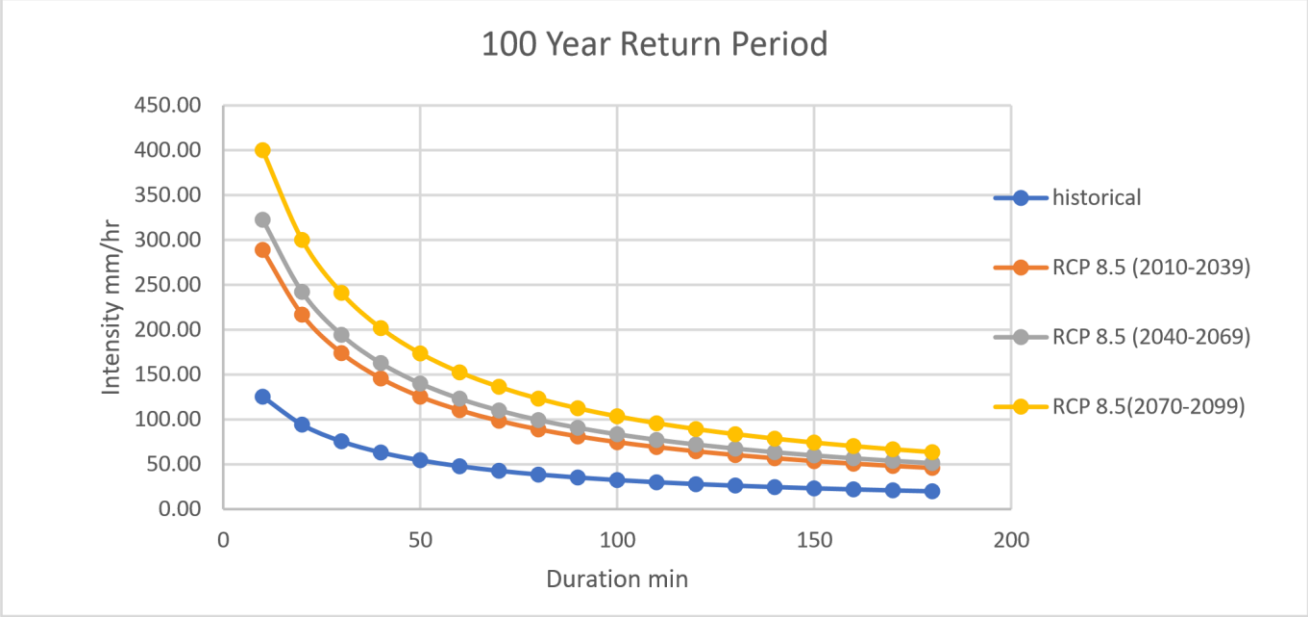
100 Year Return Period
Intensity mm/hr
450.00
400.00
350.00
300.00
250.00
200.00
150.00
100.00
50.00
0.00
0
50
100
150
200
Duration min
historical
RCP 8.5 (2010-2039)
RCP 8.5 (2040-2069)
RCP 8.5(2070-2099)